Cell Reports

Article

Prostaglandin E_2 amplifies IL-17 production by γδ T cells during barrier inflammation

Graphical abstract

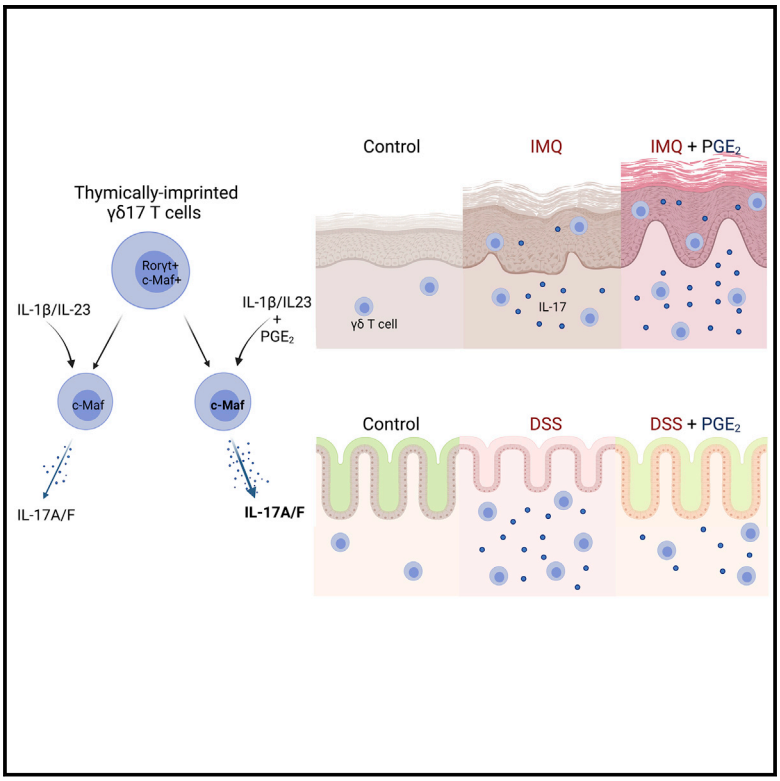

Authors

Barbara Polese, Bavanitha Thurairajah, Hualin Zhang, ..., Sabah N.A. Hussain, Valerie Abadie, Irah L. King

Correspondence

irah.king@mcgill.ca

In brief

Polese and Thurairajah et al. demonstrate that the lipid mediator prostaglandin E_2 enhances IL-17 secretion by murine γδ T cells and amplifies psoriasiform inflammation while limiting colitis severity. Their results suggest a tissue-specific role for PGE_2 production in regulating γδ17 T cell responses and pathological inflammation at barrier sites.

Highlights

- PGE_2 potently enhances IL-17 production by thymically imprinted γδ17 T cells
- PGE_2 supplementation amplifies IL-17-dependent psoriasiform inflammation
- Loss of mPGES1-dependent PGE_2 compromises intestinal γδ17 T cell responses
- γδ17 T cell activation during DSS requires commensal gut microbiota

Polese et al., 2021, Cell Reports *36*, 109456
July 27, 2021
https://doi.org/10.1016/j.celrep.2021.109456

CellPress

Cell Reports

CellPress
OPEN ACCESS

Article

Prostaglandin E_2 amplifies IL-17 production by γδ T cells during barrier inflammation

Barbara Polese,[1,4,6] Bavanitha Thurairajah,[1,2,6] Hualin Zhang,[1,2] Cindy Leung Soo,[2,5] Clara A. McMahon,[1,2] Ghislaine Fontes,[1,2] Sabah N.A. Hussain,[1] Valerie Abadie,[3] and Irah L. King[1,2,7,*]

[1]Meakins-Christie Laboratories, Department of Medicine, McGill University Health Centre, Montreal, QC H4A 3J1, Canada
[2]McGill Interdisciplinary Initiative in Infection and Immunity, Department of Microbiology and Immunology, McGill University, Montreal, QC H3A 2B4, Canada
[3]Section of Gastroenterology, Department of Medicine, University of Chicago, Chicago, IL 60637, USA
[4]Present address: GIGA Research Center, University of Liège, 4000 Liège, Belgium
[5]Present address: Centre for Outcomes Research & Evaluation, McGill University Health Centre, 5252 Blvd de Maisonneuve, W. Montreal, QC H4A 3S5, Canada
[6]These authors contributed equally
[7]Lead contact
*Correspondence: irah.king@mcgill.ca
https://doi.org/10.1016/j.celrep.2021.109456

SUMMARY

Interleukin-17 (IL-17)-producing γδ (γδ17) T cells are innate-like lymphocytes that contribute to protective anti-microbial responses but are also implicated in pathogenic inflammation at barrier sites. Understanding tissue-specific signals that regulate this subset is important to boost host defense mechanisms, but also to mitigate immunopathology. Here, we demonstrate that prostaglandin E_2 (PGE_2), a cyclooxygenase-dependent member of the eicosanoid family, directly enhances cytokine production by circulating and tissue-specific γδ17 T cells *in vitro*. Gain- and loss-of-function *in vivo* approaches further reveal that although provision of PGE_2 amplifies psoriasiform inflammation, ablation of host mPGES1-dependent PGE_2 synthesis is dispensable for cutaneous γδ17 T cell activation. By contrast, loss of endogenous PGE_2 production or depletion of the gut microbiota compromises intestinal γδ17 T cell responses and increases disease severity during experimental colitis. Together, our results demonstrate how a lipid mediator can synergize with tissue-specific signals to enhance innate lymphocyte production of IL-17 during barrier inflammation.

INTRODUCTION

γδ T cells are innate-like lymphocytes that contribute to inflammation in diverse settings of infection and immunity (Papotto et al., 2017b). Within barrier tissues such as the skin, gut, and lung, a subset of γδ T cells are long-lived, tissue-resident cells that express the lineage-specific transcription factor Rorγt, endowing them with the ability to produce interleukin (IL)-17A, IL-17F, and IL-22 upon T cell receptor (TCR) engagement or cytokine stimulation (Papotto et al., 2017b). Although γδ T cells that secrete IL-17 (referred to hereafter as γδ17 T cells) share several properties with their IL-17-producing CD4+ αβ T cell (Th17) counterparts, important differences remain. For example, while polarization of naive CD4+ T cells into Th17 effectors is restricted to the secondary lymphoid organs, Rorγt expression and the acquisition of IL-17-producing potential by murine γδ T cells is thymically imprinted during early life (Jensen et al., 2008; Ribot et al., 2009). However, we and others have shown that under certain inflammatory conditions, *de novo* generation of γδ17 T cells also can occur in adulthood (Muschaweckh et al., 2017; Zhang et al., 2019; Papotto et al., 2017a). Regardless of ontogeny, inflammatory cytokines—most notably, IL-1 and IL-23—produced by macrophages and dendritic cells upon pattern recognition receptor engagement are sufficient for the activation of γδ17 T cells, as innate production of IL-17 within non-lymphoid tissues does not require engagement with cognate antigen (Papotto et al., 2017b). As such, γδ17 T cells are early responders to infection and tissue injury and provide protective anti-bacterial and anti-fungal immune responses in the gut and skin (Kashem et al., 2015; Cho et al., 2010; Sheridan et al., 2013; Chen et al., 2020). However, they have also been implicated in pathogenic processes such as psoriasis and fatty liver disease (Li et al., 2017; Cai et al., 2011).

Although cytokine signaling is a potent mechanism of activation, cell-intrinsic microbial and metabolite sensing can synergistically accentuate the γδ17 T cell effector program. For example, γδ17 T cells express Toll-like receptors, and stimulation with pathogen-associated molecular patterns in the presence of IL-23 amplifies IL-17 production (Martin et al., 2009). In addition, aryl hydrocarbon receptor ligands that are generated by metabolism of cruciferous vegetables or xenobiotics by the gut microbiota amplify IL-17A and IL-22 production by γδ T cells in models of microbial peritonitis (Martin et al., 2009). In contrast, stimulation with the vitamin A metabolite, retinoic acid, in the presence

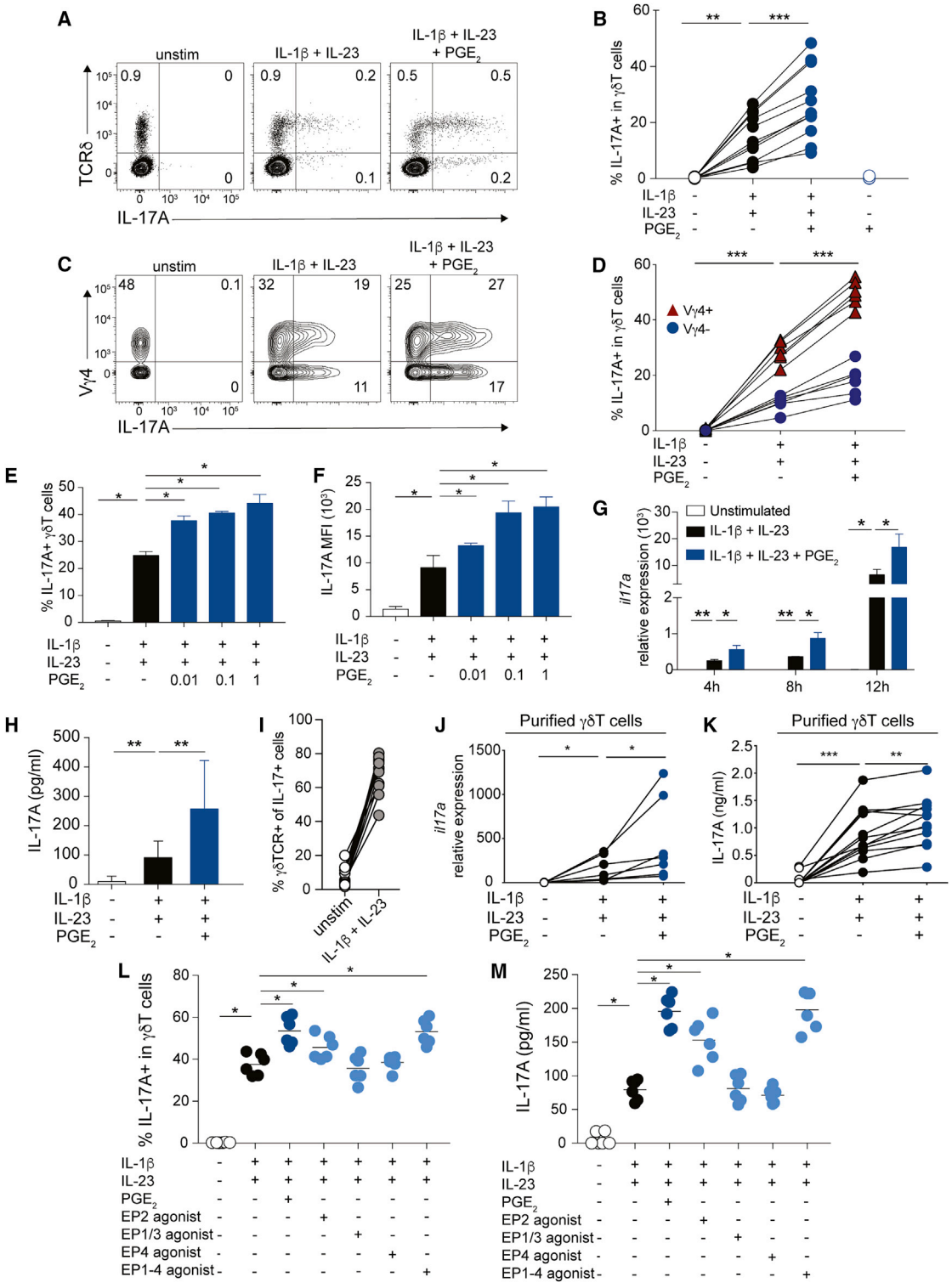

Figure 1. PGE_2 potentiates IL-17A production by γδ T cells

(A and B) Representative contour plots (A) and frequency (B) of IL-17A$^+$ cells in live γδTCR$^+$CD3$^+$ LN cells following 18 h of culture under the indicated conditions.

(C) Representative contour plots of Vγ4 and IL-17A in CD3$^+$TCRδ$^+$ LN cells following 18 h of culture under the indicated conditions.

(D) The frequency of IL-17A$^+$ cells among Vγ4$^+$ and Vγ4$^-$ γδ T cells stimulated as in (C).

(E and F) The frequency (E) and MFI (F) of IL-17A$^+$ cells among γδ T cells stimulated under the indicated conditions.

(legend continued on next page)

of IL-1β and IL-23 decreases production of IL-17 by Rorγt+ γδ T cells while increasing IL-22 secretion (Mielke et al., 2013). Thus, elucidating the repertoire of tissue-specific amplifiers of γδ17 T cells is fundamental to understanding their relevance to health and disease.

Prostaglandin E_2 (PGE_2) is a member of the eicosanoid family of lipid mediators that exerts pleiotropic functions on host cells during infection and inflammation (Kalinski, 2012). A product of phospholipid-derived arachidonic acid metabolism, PGE_2 synthesis depends on a series of enzymatic reactions including cyclooxygenase-dependent production of prostaglandin H_2 that is further modified by prostaglandin E synthases cPGES1 and mPGES1 (Kalinski, 2012). While cPGES1 is responsible for basal production of PGE_2, mPGES1 is inducible by infection and tissue damage and is the dominant mediator of PGE_2 synthesis during inflammation. Although PGE_2 can signal via four E type prostanoid receptors (EP1–EP4), hematopoietic cells predominantly express EP2 and EP4 (Kalinski, 2012). For example, PGE_2 has been shown to enhance IL-17 production by mouse and human αβ CD4+ T cells (Th17 cells) via EP2 and EP4 signaling (Chizzolini et al., 2008; Boniface et al., 2009; Napolitani et al., 2009; Yao et al., 2009). However, Valdez et al. (2012) showed an inhibitory effect of PGE_2 on Th17 development. This work was followed by a study demonstrating that mice lacking EP2/EP4 in αβ T cells were protected from imiquimod-induced inflammation, a model of psoriasis that requires cutaneous IL-17 production (Lee et al., 2019). Additionally, a PGE_2-EP4 axis enhanced production of IL-22 by Rorγt-expressing type 3 innate lymphoid cells (ILC3s) in sepsis models and experimental colitis (Duffin et al., 2016). Despite its clear importance in Rorγt-expressing cell function, the specific contribution of PGE_2 to γδ17 T cell function remains largely unknown. Given the cell-specific nature of PGE_2 function, we examined two models of cutaneous and intestinal barrier inflammation to reveal tissue-specific effects of this lipid in amplifying the γδ17 T cell effector program.

RESULTS AND DISCUSSION

PGE_2 enhances IL-17 production by γδ T cells *in vitro*

To test a potential effect of PGE_2 on IL-17 production by γδ T cells, single-cell suspensions were generated from the peripheral lymph nodes (LNs) of unmanipulated C57BL/6 mice and cultured with IL-1β and IL-23 in the presence or absence of the lipid mediator. Consistent with previous studies (Sutton et al., 2009), IL-1β and IL-23 significantly increased production of IL-17A by γδ T cells after 18 h of stimulation (Figures 1A and 1B). Notably, the addition of PGE_2 significantly amplified the frequency of IL-17A$^+$ γδ T cells over cytokine stimulation alone (Figured 1A and 1B). However, PGE_2 alone had no effect (Figure 1B). Using the Tonegawa nomenclature, this effect was not limited to Vγ4$^+$ γδ T cells, a thymically imprinted subset with IL-17-producing potential (Gray et al., 2013), as both Vγ4$^+$ and Vγ4$^-$ γδ T cell subsets increased cytokine production in response to PGE_2 exposure (Figures 1C and 1D). PGE_2 acted in a potent manner, as only 0.01 μM of the lipid significantly increased the frequency and magnitude of cytokine-stimulated IL-17A$^+$ γδ T cells (Figures 1E and 1F). PGE_2 also rapidly increased *Il17a* transcription and secretion in T cell cultures (Figures 1G and 1H). As γδ T cells comprised the majority of IL-17A$^+$ cells following IL-1β and IL-23 stimulation, these data likely represent changes in the γδ T cell population (Figure 1I). Consistent with this interpretation, PGE_2 similarly increased *Il17a* transcription and IL-17A secretion from purified γδ T cells stimulated with IL-1β and IL-23 (Figures 1J and 1K). In order to identify the relevant receptor(s) mediating this effect, we used agonists targeting EP receptors, the known PGE_2 receptor family. While EP3 and EP4 agonists had no effect on IL-17A production, an EP2 agonist, as well as misoprostol—a synthetic PGE_2 analog with promiscuous EP receptor binding activity—recapitulated the PGE_2 effect (Figures 1L and 1M). Furthermore, EP2 was moderately, but broadly, expressed by lymph-node-derived γδ T cells (Figure S1), supporting our functional data that PGE_2 increases IL-17A production by γδ T cells predominantly through the EP2 receptor. Altogether, these results show that a PGE_2-EP2 pathway directly amplifies the γδ17 effector program.

PGE_2 acts on committed γδ17 cells to enhance cytokine-mediated activation

Differential TCR signaling during thymic selection imprints non-overlapping effector programs on γδ T cells characterized by expression of Rorγt or T-bet and potential for IL-17 or IFNγ production, respectively (Muñoz-Ruiz et al., 2016). Imprinted γδ T cells seed non-lymphoid tissues in early life, are long-lived, express CD44, and are largely maintained by self-renewal *in situ*. By contrast, the majority of circulating γδ T cells found in the spleen and LNs lack CD44 expression and do not express lineage-restricted transcription factors. However, inflammatory signals—most notably, IL-23 stimulation—can drive phenotypically "naive" γδ T cells to undergo *de novo* differentiation into Rorγt$^+$ IL-17-producing γδ T cells (Muschaweckh et al., 2017; Papotto et al., 2017a). Considering these unique properties of γδ T cells, we investigated whether PGE_2 (1) was required for steady-state generation of γδ17 cells, (2) synergizes with TCR signals to amplify IL-17 production, and/or (3) promotes *de novo* γδ17 T cell differentiation. To address the role of PGE_2 in steady-state γδ17 T cell generation, we assessed the frequency

(G) *Il17a* mRNA expression in T cell cultures stimulated as indicated for 4, 8, or 12 h.
(H) IL-17A secretion by T cells cultured as indicated.
(I) The frequency of TCRδ+ cells within the total IL-17A$^+$ population in unstimulated or IL-1β and IL-23 stimulated conditions.
(J and K) *Il17a* mRNA expression (J) and IL-17A secretion (K) from purified γδ T cells cultured under the indicated conditions.
(L and M) The frequency of IL-17A$^+$ cells among γδ T cells (L) and IL-17A secretion from LN T cells (M) stimulated under the indicated conditions in the presence or absence of Butaprost (EP2 agonist), Sulprostone (EP1/EP3 agonist), AH23848 (EP4 agonist), and Misoprostol (EP1-4 agonist).
(B, D, and I–M) Each dot represents cells from an individual mouse, and (B, D, and I–K) each line represents cells from an individual mouse. (A and C) Contour plots are representative at least three independent experiments. Numbers indicate frequency of cells within each quadrant. (E–H) Data are represented as mean with SD. Graphs are pooled data from at least two independent experiments with n = 3 in each experiment. Data were analyzed using the Wilcoxon nonparametric paired t test (*$p < 0.05$, **$p < 0.01$, ***$p < 0.001$). See also Figure S1.

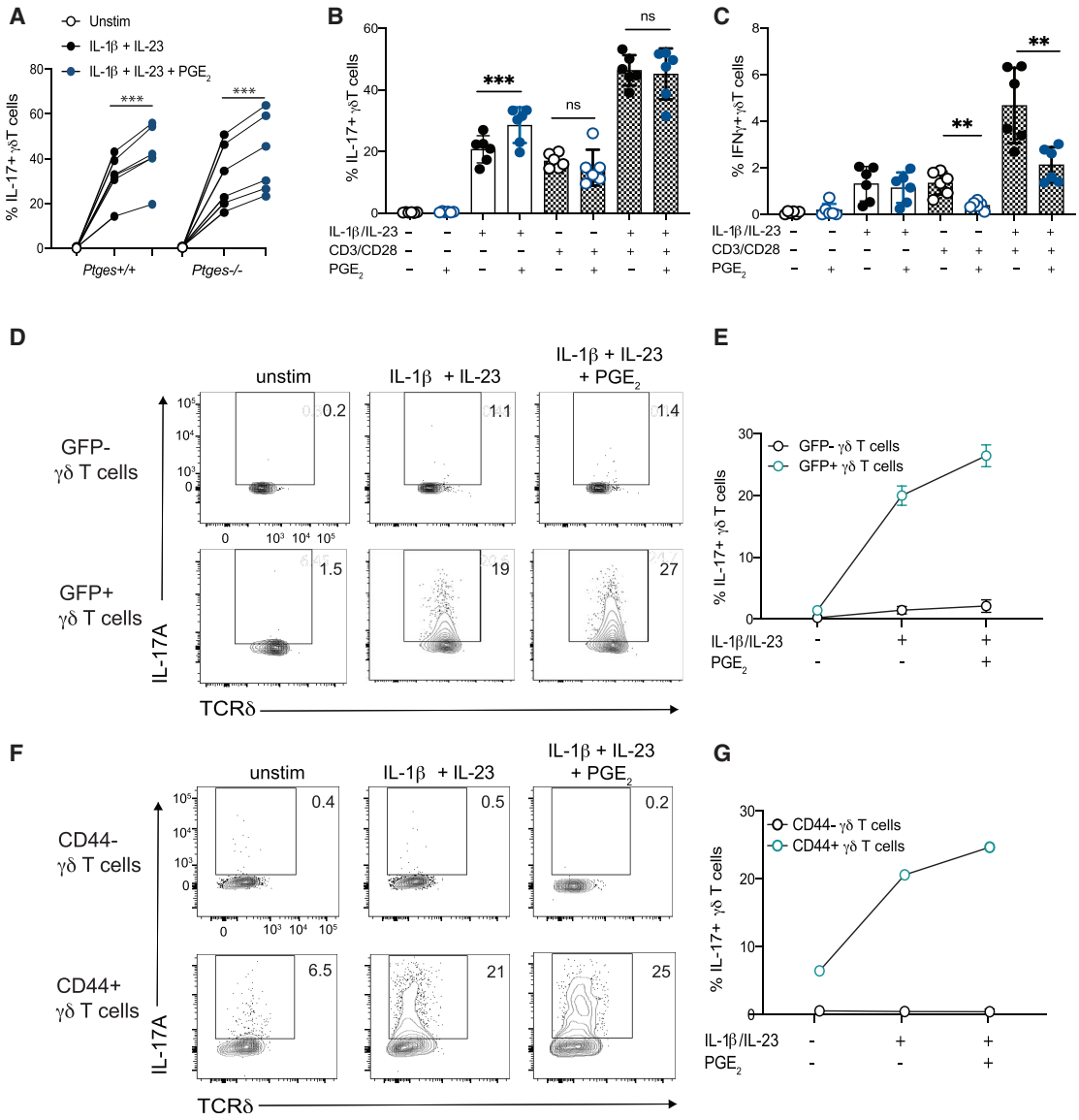

Figure 2. PGE_2 enhances cytokine-mediated activation of committed γδ17 T cells

(A) The frequency of IL-17A$^+$ cells among γδ T cells in single-cell suspensions from the skin-draining LNs of *Ptges*$^{+/+}$ and *Ptges*$^{-/-}$ mice following 18 h of culture as indicated.

(B and C) The frequency of IL-17A$^+$ (B) and IFNγ$^+$ (C) cells among γδ T cells stimulated for 18 h under the indicated conditions.

(D and E) Representative contour plots (D) and frequency (E) of IL-17A$^+$ cells among γδ T cells in sorted GFP- (Rorγt$^-$) CD3$^+$ cells and GFP$^+$ (Rorγt$^+$) CD3$^+$ cells following 4 h of culture in conditions indicated. Numbers indicate the frequency of cells within each quadrant.

(F and G) Representative contour plots (F) and frequency (G) of IL-17A$^+$ cells among γδ T cells in sorted CD44$^-$CD62L$^+$ γδ T cells and CD44$^-$CD62L$^+$ γδ T cells following 5 days of culture in conditions indicated.

(A–C) Each dot represents cells from an individual mouse. Graphs are pooled data from at least two independent experiments with n = 3 in each experiment. Data were analyzed using the Wilcoxon nonparametric paired t test (*p < 0.05, **p < 0.01, ***p < 0.001). (E and G) Graphs are pooled data from at least two independent experiments with cells pooled from 3–5 mice with n = 2.

and number of Rorgγt$^+$ γδ17 T cells in the LNs of mice lacking microsomal prostaglandin E synthase (mPGES1; encoded by *Ptges*), the enzyme required for inducible PGE_2 production (Montrose et al., 2015). Compared to *Ptges*$^{+/+}$ littermate controls, the frequency and number of Rorγt$^+$ IL-17$^+$ cells were similar between groups (Figure 2A). To test the impact of PGE_2 on TCR-mediated production of IL-17A by γδ T cells, LN cells from wild-type (WT) mice were stimulated with anti-CD3 and anti-CD28 in the presence or absence of PGE_2 and IL-17 polarizing cytokines. Similar to results shown in Figure 1, PGE_2 enhanced IL-17A production during IL-1β and IL-23 stimulation (Figure 2B). By contrast, PGE_2 had no impact on γδ T cell

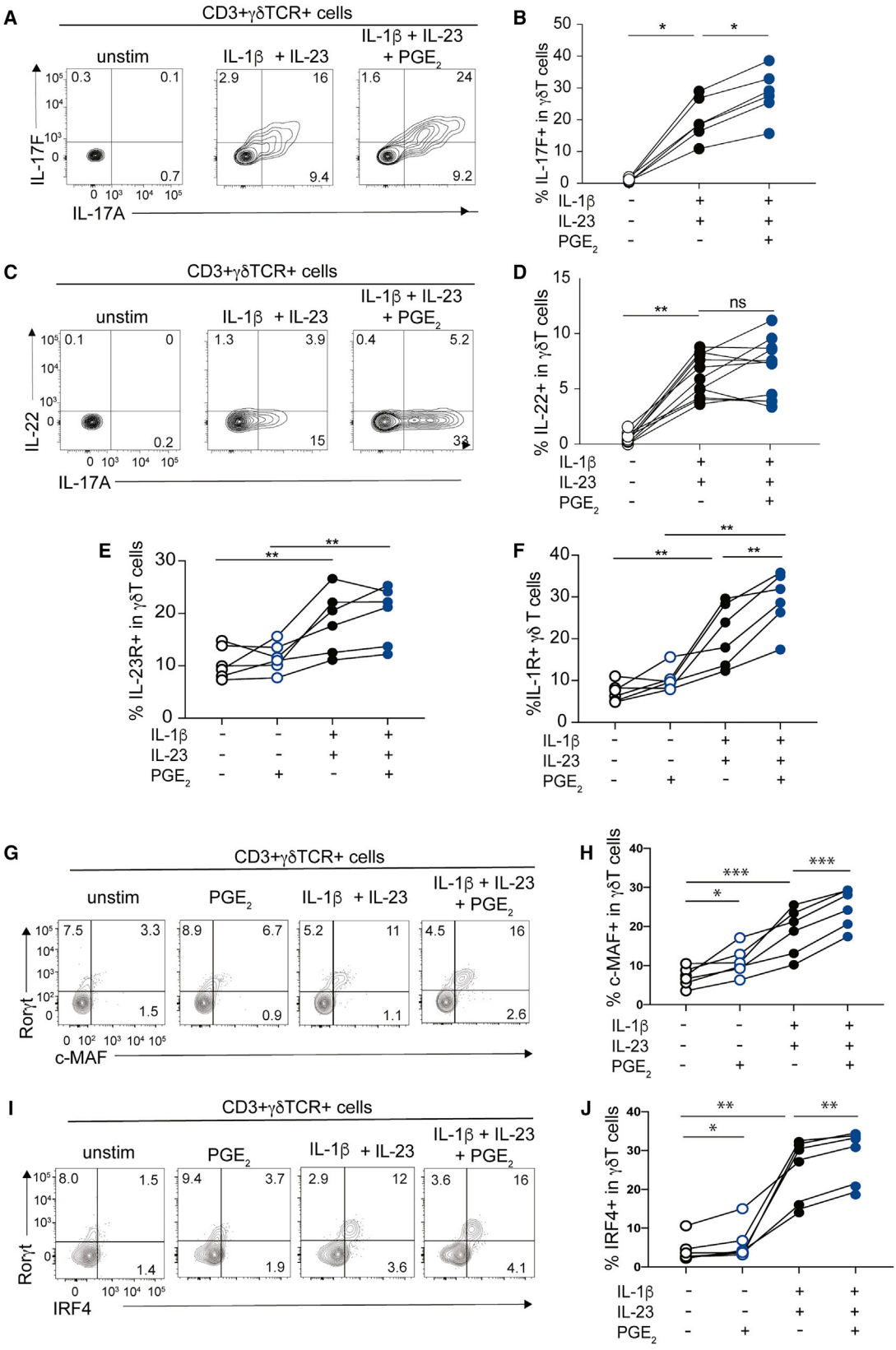

(legend on next page)

production of IL-17A during TCR-mediated activation (Figure 2B) but, interestingly, inhibited interferon (IFN)γ production by γδ T cells under these conditions (Figure 2C).

We next tested whether PGE_2 may impact *de novo* differentiation of γδ17 T cells. For these studies, we took two approaches. First, we fluorescence-activated cell sorting (FACS) purified GFP^+ and GFP^- T cells from the LNs of $Ror\gamma t^{GFP/+}$ mice that express GFP in place of the endogenous Rorγt gene and stimulated each subset with IL-1β and IL-23 in the presence or absence of PGE_2 prior to quantifying IL-17 production 4 h later. Purified GFP+ γδ T cells rapidly produced IL-17A in response to cytokine stimulation, and this response was increased by PGE_2 (Figure 2D). However, GFP^- γδ T cells produced minimal IL-17A under either condition and were not increased by PGE_2 treatment (Figure 2D). As a second approach, we adopted a previously published protocol demonstrating that anti-CD3/CD28 stimulation of naive $CD44^-$ γδ T cells, in combination with IL-1β and IL-23, over several days of culture induces *de novo* IL-17 production (Muschaweckh et al., 2017). Although PGE_2 increased the production of IL-17A by $CD44^+$ γδ T cells following extended culture with cytokines, we were unable to detect IL-17A production following combined TCR and cytokine stimulation of $CD44^-$ γδ T cells by intracellular cytokine staining (Figure 2E) or ELISA (not shown). It currently remains unclear why were not able to effectively generate *de novo* γδ17 T cells as previously described. Nevertheless, our data demonstrate that under the conditions tested, PGE_2 selectively promotes IL-17 production from committed γδ T cells in the context of inflammatory cytokine signals.

Cytokine-dependent and cytokine-independent effects of PGE_2 on the γδ17 effector program

To further investigate PGE_2 effects on γδ T cells, we measured other cytokines known to be produced by $IL\text{-}17A^+$ γδ T cells, including IL-17F and IL-22. Indeed, PGE_2 amplified IL-17F production by γδ T cells (Figures 3A and 3B). In contrast, IL-22 production was not amplified by PGE_2 under cytokine (Figures 3C and 3D) or TCR-mediated activation (Figure S2), a result that has been similarly observed in $CD4^+$ T cells (Boniface et al., 2009). Previous studies also showed that PGE_2 increases IL-1 and IL-23 receptor expression by naive human $CD4^+$ T cells (Boniface et al., 2009). Although we were unable to detect any upregulation of these receptors in response to PGE_2 alone, PGE_2 stimulation in combination with cytokine treatment did lead to an increase in IL-1R expression (Figures 3E and 3F). Production of IL-17 by diverse cell lineages has been universally shown to require expression of the transcription factor Rorγt. In addition, the co-factors c-Maf and IRF4 have been implicated in the development and/or effector functions of γδ17 T cells (Zuberbuehler et al., 2019; McKenzie et al., 2017). Notably, both c-Maf and IRF4 were significantly increased in $Ror\gamma t^+$ γδ T cells following cytokine stimulation, and PGE_2 further increased the frequency of cells expressing both transcription factors (Figures 3G–3J). Interestingly, treatment of cells with PGE_2 alone induced a small, but significant, increase in c-Maf and, to a lesser extent, IRF4 expression, suggesting that this lipid mediator may stabilize and/or enhance γδ17 cell effector function through regulation of these transcription factors independent of cytokine stimulation. Collectively, our results indicate that PGE_2 promotes a focused effector phenotype in γδ17 T cells, most notably via enhanced expression of IL-1R and c-Maf.

PGE_2 exacerbates, but is not required for, inflammatory cutaneous γδ17 cell responses

Our initial studies focused on the impact of PGE_2 on circulating γδ17 T cell responses. However, the majority of this subset resides in non-lymphoid tissues, such as the skin and gut, and have developmental and functional properties distinct from their lymphoid counterparts (Polese et al., 2020). To test whether PGE_2 could amplify cutaneous γδ17 T cell responses, we used an approach developed by Ridaura et al. (2018) in which topical application of the commensal microbe *Corynebacteria accolens* (*C. accolens*) increases the number of $V\gamma4^+$ γδ17 T cells in the skin of mice. As previously described, *C. accolens* application led to a robust increase in the frequency of $IL\text{-}17^+$ γδ T cells in the skin of WT mice (Figures 4A and 4B). However, *C. accolens* colonization induced a similar number of $V\gamma4^+$ and $V\gamma4^-$ γδ17 T cells in $Ptges^{-/-}$ mice compared to littermate controls (Figures 4A and 4B). These results indicate that mPGES-1-dependent PGE_2 production is dispensable for γδ17 T cell responses to *C. accolens* exposure. As PGE_2 is considered an "inflammatory" eicosanoid, and *C.accolens*-mediated enhancement of γδ17 cells occurs in the absence of patent inflammation (Ridaura et al., 2018), we questioned whether PGE_2 may play a more important role in γδ17 T cell responses during a pathological inflammatory response. To this end, we treated $Ptges^{+/+}$ and $Ptges^{-/-}$ littermates with topical imiquimod (IMQ), a TLR7/8 agonist that stimulates γδ17 T-cell-dependent psoriasiform inflammation (Sandrock et al., 2018; Cai et al., 2011). However, ear swelling, acanthosis, and γδ17 T cell responses were similar between IMQ-treated groups (Figures 4C–4G), despite a significant decrease in PGE_2 production from skin extracts as well as *in vitro* stimulation of bone-marrow-derived macrophages from $Ptges^{-/-}$ mice (Figures S3A and S3B). Consistent with these results, *ex vivo* stimulation of dermal γδ17 T cells from naive mice with PGE_2 did not increase IL-17 production (Figure 4H), even

Figure 3. Cytokine-dependent and cytokine-independent effects of PGE_2 on the γδ17 T cell effector program

(A and B) Representative contour plots of IL-17F and IL-17A expression (A) and frequency of $IL\text{-}17F^+$ cells (B) in $CD3^+TCR\delta^+$ LN cells following 18 h of culture under the indicated conditions.

(C and D) Representative contour plots (C) and frequency (D) of IL-22 expression in $CD3^+TCR\delta^+$ LN cells following 18 h of culture under the indicated conditions.

(E and F) The frequency of IL-23R (E) and IL-1R (F) expression among γδ T cells following 18 h after stimulation under the indicated conditions.

(G–J) Representative contour plots (G and I) and frequency (H and J) of c-Maf and IRF4 expression in relation to RORγt in γδ T cells under the indicated conditions.

(A, C, G, and I) Contour plots shown in are representative of three independent experiments, and numbers indicate the frequency of cells within each quadrant.

(B, D–F, H, and J) Graphs are pooled data from two independent experiments with n = 3 in each experiment, and each line represents cells from an individual mouse. Data analyzed using the Wilcoxon nonparametric paired t test (*$p < 0.05$, **$p < 0.01$, ***$p < 0.001$). See also Figure S2.

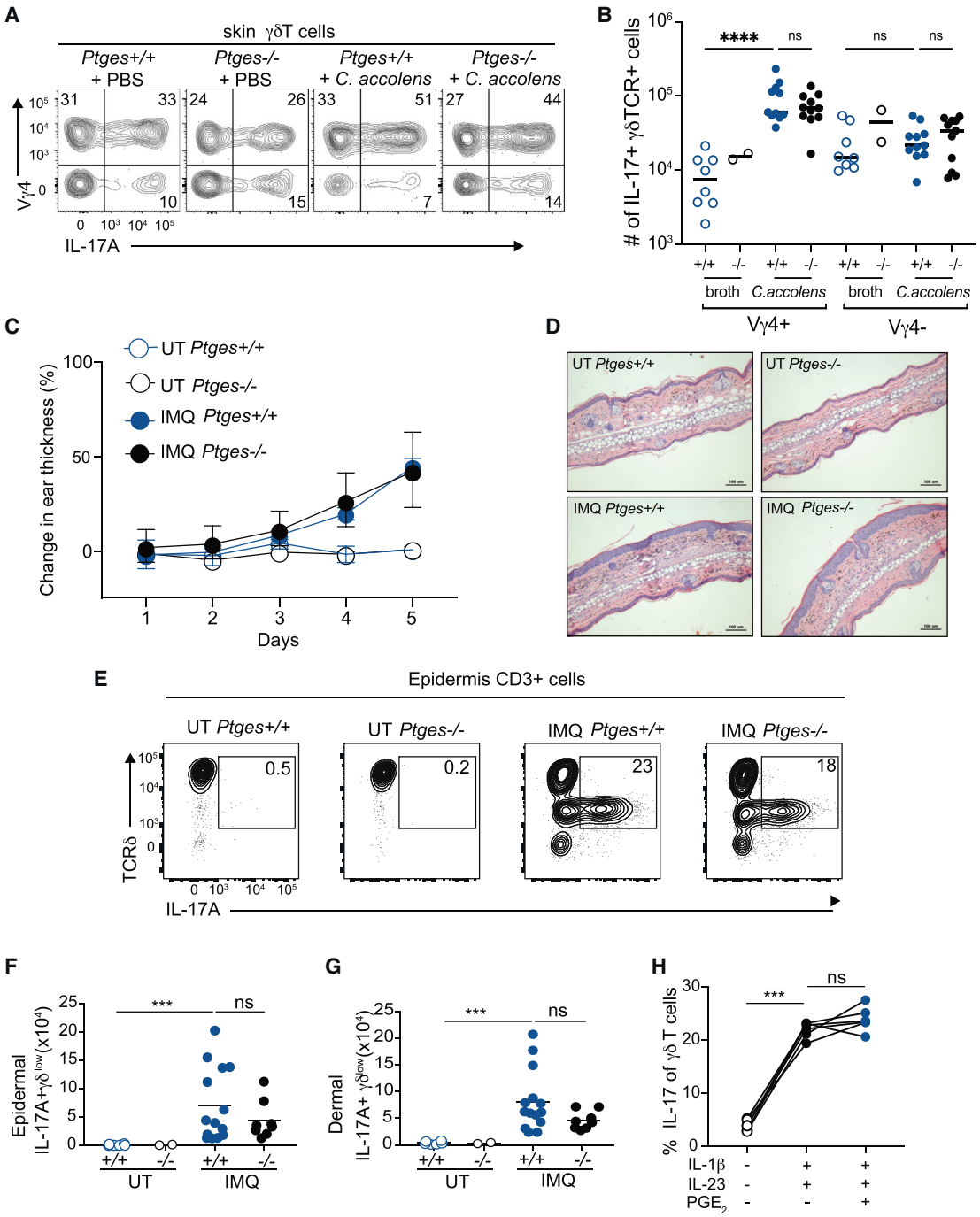

Figure 4. PGE_2 exacerbates, but is not required for, inflammatory cutaneous γδ17 T cell responses

(A and B) Representative contour plots (A) and absolute number (B) of IL-17A$^+$ Vγ4$^+$ and Vγ4$^-$ among cutaneous γδ T cells (viable CD45$^+$CD3$^+$TCRδ^{low} cells) isolated from the skin of *Ptges*$^{+/+}$ and *Ptges*$^{-/-}$ littermates topically administered *C. accolens* or control (sterile broth).

(C) Change in ear thickness (compared to day 0) in untreated or IMQ-treated *Ptges*$^{+/+}$ or *Ptges*$^{-/-}$ mice, monitored daily; three independent experiments (n = 4–24/group).

(D) Representative H&E-stained sections of skin from mice described in (C). Scale bar, 100 μm.

(E) Representative contour plots showing the expression of IL-17A and TCRδ among T cells in the epidermis of untreated versus IMQ-treated *Ptges*$^{+/+}$ and *Ptges*$^{-/-}$ littermates. Data shown represent *ex vivo* cytokine production without additional stimulation.

(F and G) Absolute counts of IL-17A-producing γδ T cells isolated from the epidermis (F) and dermis (G) of untreated and IMQ-treated *Ptges*$^{+/+}$ and *Ptges*$^{-/-}$ mice.

(H) Proportion of IL-17A$^+$ γδ T cells from total skin cells isolated from untreated B6 mice and stimulated for 4 h under the indicated conditions.

(legend continued on next page)

though we were able to detect expression of EP2 in all cutaneous γδ T cell subsets (Figure S1). These results contrast with a previous study showing that genetic deletion or blockade of EP2 and EP4 signals in T cells attenuated IMQ-induced ear swelling (Lee et al., 2019). These disparate results may be explained by compensatory increases in other prostanoids that signal through EP2 and EP4 or the genetic models employed (Fiala et al., 2019). Therefore, we took a gain-of-function approach by injecting a stable form of PGE_2 (16,16-dimethyl-PGE_2) into C57BL/6 mice during IMQ application. As shown in Figure 5A, systemic PGE_2 administration in the context of IMQ treatment to the back skin of mice qualitatively increased the red, scaly lesions on IMQ-treated, but not untreated, skin. For a more quantitative assessment, we applied IMQ to the ear skin of control or PGE_2-treated mice. Similarly, IMQ-induced ear thickening was significantly increased in PGE_2-injected mice compared to control-treated animals (Figures 5B and C). As we and others have previously demonstrated, accumulation of epidermal γδ17 T cells is a key feature of IL-17-dependent psoriasiform inflammation (Mabuchi et al., 2013; Sandrock et al., 2018; Zhang et al., 2019). PGE_2 treatment was associated with a greater accumulation of epidermal, but not dermal, γδ17 T cells (Figures 5D–5G). The ability of PGE_2 to aggravate IMQ-induced skin pathology despite a lack of an effect on *ex-vivo*-stimulated cutaneous γδ T cells suggested that this lipid may also enhance inflammation via effects on other immune and/or structural cell compartments. Notably, PGE_2 has been shown to increase production of IL-23, a cytokine required for psoriasiform inflammation (van der Fits et al., 2009; Sheibanie et al., 2004), but also promote T regulatory cell (Treg) development as well as IL-10 expression (Baratelli et al., 2005; Huang et al., 1996). However, no detectable differences in cell types associated with their production—namely, dendritic cells or Foxp3+ Tregs—was observed between the groups (Figures S4A and S4B). PGE_2 has also been shown to increase blood vessel dilation through combined action on the vascular endothelium as well as neutrophil recruitment (Hellewell et al., 1992; Wedmore and Williams, 1981). Consistent with these functions, PGE_2 administration led to a rapid swelling of the ear vasculature in the absence and presence of IMQ treatment (Figures S4C and S4D) and a variable, but significant decrease in blood oxygen levels (Figure S4F) compared to vehicle-treated animals. In addition, PGE_2 treatment increased IMQ-dependent dermal neutrophil recruitment and *Il1b* expression compared to IMQ treatment alone (Figures S4G and S4H). Collectively, these results indicate that PGE_2 enhances IMQ-mediated inflammation by multiple mechanisms—including, but not limited to, the γδ17 T cell program.

Loss of mPGES1-dependent PGE_2 synthesis compromises intestinal γδ17 T cell activation and exacerbates DSS-induced colitis

Given that endogenous PGE_2 production was dispensable for γδ17 T cell responses in the context of psoriasiform inflammation, we next tested whether this lipid mediator contributed to γδ17 T cell activation in a different setting of barrier inflammation. We chose to use the dextran sulfate sodium (DSS) model of colitis because in this setting, (1) PGE2 has been shown to enhance epithelial proliferation and tissue repair (Brown et al., 2007; Montrose et al., 2015) and to be highly produced in colonic tissue (Figure S3C); (2) γδ T cell-derived IL-17 enhances intestinal barrier integrity (Lee et al., 2015); and (3) *ex vivo* stimulation of colonic lamina propria cells with IL-1β and IL-23 potently induced IL-17A production by γδ T cells, a result that was significantly enhanced in the presence of PGE_2 (Figure 6A). Consistent with these data, γδ T cells expressed the EP2 receptor (Figure S1), and analysis of cytokine production in the absence of *in vitro* restimulation revealed that they were the dominant IL-17A-producing cell type in the colon during DSS treatment compared to $CD4^+CD3^+$ T cells and $CD127^+CD3^-$ ILCs (Figures 6B and 6C), a response that peaked after 5 days of treatment (Figures 6B and 6C). For comparison, we assessed IL-22 production, as previous studies have found this cytokine to be important for protection against DSS, and it can be produced by γδ T cells (Duffin et al., 2016). We found that ILCs were the dominant source of this cytokine under both steady-state and inflammatory conditions (Figure 6D). To test whether the loss of mPGES1-dependent PGE_2 production had an impact on these responses, $Ptges^{+/+}$ and $Ptges^{-/-}$ littermates were treated for 5 days with 3% DSS in the drinking water. Based on the kinetics of the IL-17 and IL-22 response (Figures 6B and 6C), we chose to examine the day 5 time point. Although mice were only beginning to lose weight within this time frame (Figure 6E), $Ptges^{-/-}$ mice exhibited increased intestinal bleeding and severe villus erosion, confirming a previously reported role for PGE_2 in supporting epithelial barrier integrity (Figures 6F and 6G) (Montrose et al., 2015). Furthermore, increased host morbidity correlated with a decrease in the number of colonic γδ17 T cells compared to DSS-treated littermate controls (Figure 6H). By contrast, no defect in IL-22 production by ILCs was observed (Figure 6I). The altered inflammatory response in $Ptges^{-/-}$ mice was further confirmed by a decreased number of $CD11b^+Ly6G^+$ neutrophils isolated from colon lamina propria (Figure 6J), a population responsive to IL-17-driven chemokine production (Cua and Tato, 2010).

Given the critical role of IL-10 in limiting disease severity in both human inflammatory bowel disease (IBD) and murine models of colitis, as well as the ability of PGE_2 to promote IL-10 production (Shouval et al., 2014, Medeiros et al., 2009), we assessed expression of this cytokine by qPCR from total tissue as well as intracellular cytokine staining of macrophage and $Foxp3^+$ Tregs. While we were unable to obtain high-quality RNA from the inflamed colon (Viennois et al., 2013), intracellular cytokine staining revealed variable changes in gut-macrophage-derived IL-10. In contrast, we observed a consistent and significant increase in intestinal IL-10 production from Tregs during colitis that was similar between $Ptges^{+/+}$ and $Ptges^{-/-}$ mice (Figure S5). Although we cannot completely exclude a role for a PGE_2-IL-10 axis in protection from colitis,

(A, B, and D–G) Data from three independent experiments containing at least 3 mice/group. (H) Pooled data from two independent experiments. Each line represents an individual mouse. Numbers indicate the frequency of cells within each quadrant or gate. (B, F, and G) Data analyzed using the Mann-Whitney nonparametric unpaired t test (**$p < 0.01$, ***$p < 0.001$; ns, not significant). (H) Data were analyzed using the Wilcoxon nonparametric paired t test (*$p < 0.05$, **$p < 0.01$, ***$p < 0.001$). See also Figure S3.

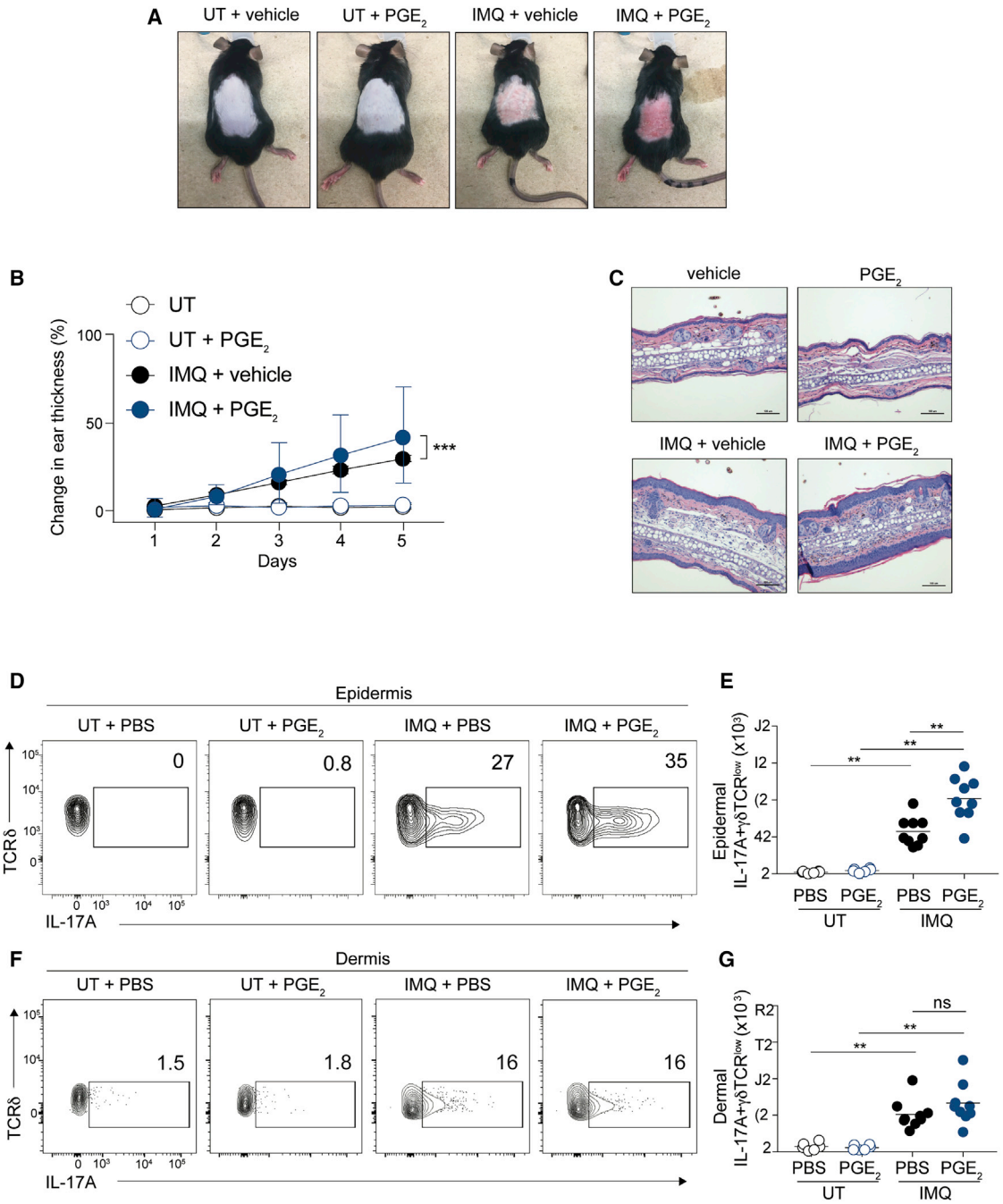

Figure 5. PGE_2 administration enhances IMQ-induced inflammation and cutaneous γδ17 T cell responses

(A) Representative images of mice treated with PBS or IMQ on their back for 5 consecutive days and intraperitoneally (i.p.) injected with stable PGE_2 (16,16-dimethyl-PGE_2) or vehicle control.

(B and C) Change in ear thickness (compared to day 0) (B) and representative H&E staining of ear skin tissue (C) of untreated or IMQ-treated B6 mice injected with 16,16-dimethyl-PGE_2 or vehicle. Scale bar, 100 μm. Three independent experiments (n = 16–24/group).

(D and E) Representative contour plots (D) and absolute number (E) of IL-17A-producing γδ T cells (viable $CD45^+CD3^+$ $TCR\delta^{low}$ $IL\text{-}17A^+$) isolated from the epidermis of untreated versus daily IMQ-treated mice injected with 16,16-dimethyl-PGE_2 or vehicle.

(F and G) Representative contour plots (F) and absolute number (G) of IL-17A-producing γδ T cells (viable $CD45^+CD3^+$ $TCR\delta^{low}$ $IL\text{-}17A^+$) isolated from the dermis of mice described in (D).

(B) Data analyzed using the 2-way ANOVA and (E and G) Mann-Whitney nonparametric unpaired t test (*$p < 0.05$, **$p < 0.01$, ***$p < 0.001$; ns, not significant). See also Figure S4.

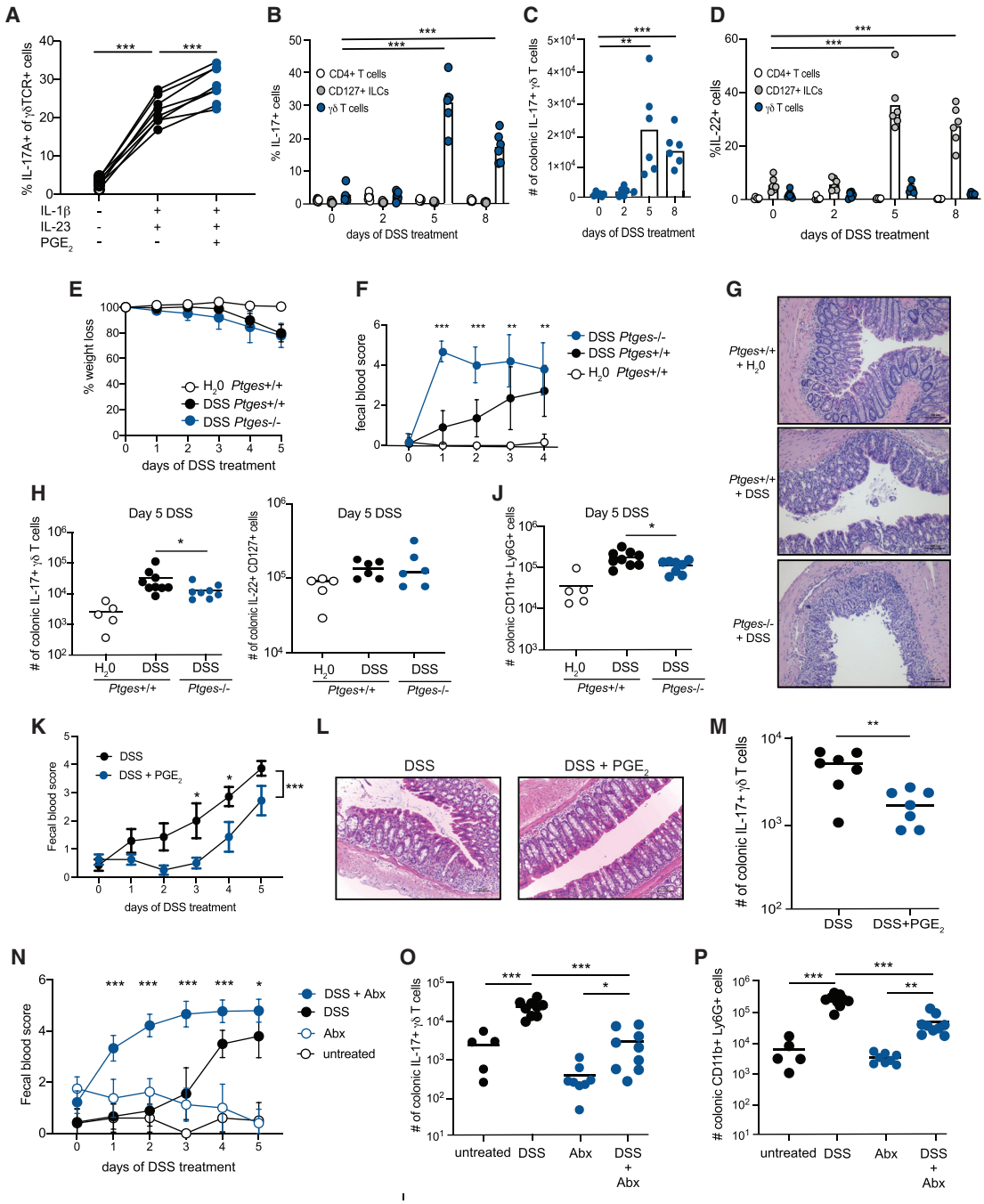

Figure 6. mPGES1 deficiency and gut microbiota depletion compromise γδ17 responses and increase the severity of DSS-induced colitis

(A) Frequency of IL-17A$^+$ γδT cells in colon cells stimulated *in vitro* for 4 h under the indicated conditions.

(B) Frequency of IL-17A$^+$ cells within the ILC (CD45$^+$CD11b$^-$B220$^-$CD3$^-$CD127$^+$) and CD4$^+$ T cells (CD45$^+$CD3$^+$CD4$^+$) and γδ T cells (CD45$^+$CD3$^+$TCRδ$^+$) populations on days 0, 2, 5, and 8 of DSS treatment. Data shown represent *ex vivo* cytokine production without additional stimulation.

(C) Absolute number of γδ17 T cells in the colon on days 0, 2, 5, and 8 of DSS treatment.

(D) Frequency of IL-22$^+$ cells within the ILC and CD4$^+$ T cells and γδ T cells populations on days 0, 2, 5, and 8 of DSS treatment.

(E–G) Change in weight (compared to day 0) (E), fecal blood assessment (F), and representative H&E staining of cross-sections of colon tissue (G) of untreated mice and DSS-treated *Ptges*$^{+/+}$ and *Ptges*$^{-/-}$ littermates. Scale bar, 100 μm. Two independent experiments (n = 5–7/group).

(H–J) Absolute number of γδ17 T cells (H), IL-22+ILCs (I), and neutrophils (CD45$^+$CD11b$^+$Ly6G$^+$) (J) in the colon of *Ptges*$^{+/+}$ and *Ptges*$^{-/-}$ littermates after 5 days of water or DSS treatment.

(K–M) Fecal blood intensity (K) and representative H&E staining of cross-sections of colon tissue (L) and absolute number of γδ17 T cells (M) in B6 mice injected with 16,16-dimethyl-PGE$_2$ or vehicle given water or DSS for 5 days. Scale bar, 100 μm. Two independent experiments (n = 7/group).

(legend continued on next page)

our results show that PGE_2 deficiency is closely associated with decreased IL-17A-producing γδ T cells in the inflamed colon and increased susceptibility to DSS-induced colitis. Finally, we performed a gain-of-function experiment in our colitis model in which we administered 16,16-dimethyl PGE_2 to WT mice during DSS administration. Daily administration of PGE_2 significantly attenuated intestinal bleeding and tissue damage induced by DSS treatment (Figures 6K and 6L). Importantly, the ability of PGE_2 treatment to prevent tissue inflammation precluded activation of lamina propria γδ17 T cells (Figure 6M).

The rapid induction of intestinal bleeding observed during DSS administration to mPGES1-deficient mice was reminiscent of the phenotype reported for similarly treated mice raised in germ-free conditions or treated with antibiotics (Abx) (Rakoff-Nahoum et al., 2004). Therefore, we hypothesized that Abx-treated mice would phenocopy the γδ17 T cell response observed in *Ptges*$^{-/-}$ mice. Indeed, we found that mice treated with a cocktail of broad-spectrum Abx for 4 weeks prior to DSS administration exhibited rapid intestinal bleeding compared to controls (Figure 6N). Furthermore, microbiota depletion was associated with significantly fewer γδ17 T cells and neutrophils after 5 days of DSS treatment compared to microbiota-replete mice (Figures 6O and 6P). The more striking impact of microbial depletion on the γδ17 T cell response compared to loss of PGE_2 synthesis during DSS-induced colitis suggests that additional microbiota-derived signals may act in concert with PGE_2 to drive innate IL-17 production (Martin et al., 2009). In addition, PGE_2 has been shown to be produced early and transiently in a model of targeted intestinal wounding, and its temporal regulation is critical for tissue repair in this context (Jain et al., 2018). Whether the same holds true in other settings of intestinal injury or infection is unknown but may explain, in part, its impact on γδ17 T cell function. Nevertheless, our results show that PGE_2 and the intestinal microbiota regulate the γδ17 T cell response and protect from experimental colitis.

Despite the identification of γδ17 T cells as an important cell type in the early stages of various inflammatory conditions (Papotto et al., 2017b; Polese et al., 2020), tissue-specific amplifiers of their effector program are not well understood. Here, we show that the inflammatory lipid mediator PGE_2 increased γδ17 T cell cytokine production *in vitro* and during barrier inflammation *in vivo*. These data are consistent with a recent study showing that human γδ T cells isolated from patients with rheumatoid arthritis increase IL-17 production in response to PGE_2 (Du et al., 2020) and the ability of PGI_2, another COX-2 dependent eicosanoid, to enhance pulmonary γδ17 T cell activation during allergic inflammation (Jaffar et al., 2011). Notably, PGE_2 enhanced only cytokine, but not TCR-mediated activation of γδ17 T cells, reinforcing this cell subset as a robust sensor of inflammatory signals independent of antigen-specific activation. We also found that PGE_2 treatment alone had the ability to increase expression of transcription factors associated with γδ17 T cell differentiation and effector function such as c-Maf and IRF4. These results suggest that this lipid mediator may "prime" γδ T cells for responsiveness to inflammatory cytokines, particularly in tissues such as the large intestine where PGE_2 is constitutively produced at high levels and is known to be rapidly induced following tissue injury (Jain et al., 2018). The importance of endogenous PGE_2 synthesis during intestinal, but not cutaneous inflammation suggests either differential induction of this eicosanoid at these barrier sites or compensation by alternative pathways in the skin. A non-mutually exclusive explanation is that differences between the cutaneous and intestinal microbiota may shape steady-state and/or inflammation-induced host eicosanoid production and subsequent IL-17 production. Although we found that *C. accolens* application to the skin of mice increased the number of γδ17 cells in a PGE_2-independent manner, the relationship between PGE_2 and the microbiota is complex and bidirectional. Indeed, *Ptges* expression is decreased in the intestine of germ-free mice compared to conventionally raised mice (Manca et al., 2020), and many commensal and pathogenic bacterial species are known to induce PGE_2 production by leukocytes as a method of immune suppression (Agard et al., 2013). Consistent with these results, loss of MyD88-dependent responsiveness to pathogen-/damage-associated molecular patterns exacerbate DSS-induced colitis, a phenotype that can be restored by provision of PGE_2 (Brown et al., 2007). Although the latter study investigated the effects of PGE_2 on the epithelium, additional targets of PGE_2 were not examined. Interestingly, indomethacin treatment (which inhibits production of PGE_2 as well as other prostaglandins) can promote changes to the microbiota that exacerbate colitis upon fecal transfer to naive animals (Crittenden et al., 2021). Whether these latter effects result from direct modulation of the microbiota remain are unknown, but *Candida* fungal species—pathobionts resident to the skin and the gut—have been shown to produce PGE_2 (Erb-Downward and Huffnagle, 2007). Combining these studies with our data showing that antibiotic-treated mice have a similar response to DSS colitis as *Ptges*$^{-/-}$ mice strongly suggests that microbial sensing by host cells promotes PGE_2 production to amplify tissue protection pathways. Whether other commensal microbes not present in our animal colony prime cutaneous γδ17 cells via PGE_2 or other PGH_2 derivatives is yet to be determined. Indeed, microbial colonization of mice increases the number of intestinal and peritoneal γδ T cells that produce IL-17 upon subsequent *in vitro* stimulation (Duan et al., 2010). Similarly, our *ex vivo* analyses determined that the gut microbiota and PGE_2 were an important determinant of IL-17 production by γδ17 cells during DSS-induced colitis.

Although γδ-T-cell-derived IL-17 has been reported to promote epithelial tight junction and barrier restoration during murine colitis formation (Lee et al., 2015), PGE_2 also acts directly on the intestinal stem cell niche to stimulate a damage-induced regenerative response (Roulis et al., 2020; Brown et al., 2007). Remarkably, we found that this treatment significantly inhibited intestinal bleeding, inflammatory leukocyte recruitment, and

(N–P) Fecal blood intensity (N), absolute number of γδ17 T cells (O), and neutrophils (P) in untreated or antibiotic (Abx)-treated B6 mice given water or DSS for 5 days. Two independent experiments (n = 5–9/group).

(A) Data analyzed using the Wilcoxon nonparametric paired t test, (B–D, H–J, M, O, and P) Mann-Whitney nonparametric unpaired t test, and (E, F, K, and N) 2-way ANOVA (*p < 0.05, **p < 0.01, ***p < 0.001). See also Figures S3 and S5.

epithelial erosion compared to PBS-treated controls (Figures 6K and 6L). Consistently, previous studies have shown that PGE_2 directly promotes intestinal epithelial repair following injury (Miyoshi et al., 2017). The direct, protective effects of PGE_2 on barrier integrity likely prevent microbial infiltration into the intestinal lamina propria, thereby negating the microbe sensing by $\gamma\delta$17 cells necessary to reveal the amplifying effects of this lipid on IL-17 production. However, future studies will need to be performed to determine the cell-intrinsic role for microbiota and/or PGE_2 stimulation of $\gamma\delta$17 T cells in this context. Collectively, these results suggest, along with other recent studies (Duffin et al., 2016; Roulis et al., 2020), that PGE_2 acts on immune *and* stromal/epithelial cell types within the intestine during colitis to enforce tissue integrity. Finally, our results provide another potential explanation why ibuprofen, a COX2 inhibitor, is contraindicated for patients with IBD.

STAR★METHODS

Detailed methods are provided in the online version of this paper and include the following:

- KEY RESOURCES TABLE
- RESOURCE AVAILABILITY
  - Lead contact
  - Materials availability
  - Data and code availability
- EXPERIMENTAL MODEL AND SUBJECT DETAILS
  - Animals
  - Bacteria
- METHOD DETAILS
  - Cell stimulation and culture
  - Skin cell isolation
  - *C. accolens* culture and administration
  - Bone marrow-derived macrophage cultures
  - Colon cell isolation
  - Imiquimod-induced skin inflammation
  - PGE_2 quantification
  - Dextran sodium sulfate treatment
  - Antibiotic treatment
  - Flow cytometry
  - Quantitative RT-PCR and ELISA
  - Histology
- QUANTIFICATION AND STATISTICAL ANALYSIS

SUPPLEMENTAL INFORMATION

Supplemental information can be found online at https://doi.org/10.1016/j.celrep.2021.109456.

ACKNOWLEDGMENTS

We thank all members of the King laboratory for their support and feedback in preparing this manuscript. We greatly appreciate the technical support of the MUHC-RI Animal Resource Division and the Histology platform. We thank the Divangahi laboratory for generously providing *Ptges*$^{-/-}$ mice. This work was supported by the Canadian Institutes of Health Research (PJT-362757). B.P. was supported by a Marie-Curie Postdoctoral Fellowship from the University of Liege, co-funded by the European Union and a World Excellence Fellowship from Wallonie-Bruxelles International. B.T. is supported by Fonds de Recherche Santé Quebec scholarship. H.Z. is supported by a China Research Council scholarship. I.L.K. holds a Canada Research Chair in Barrier Immunity.

AUTHOR CONTRIBUTIONS

B.P. and B.T. designed and performed experiments, analyzed data, and wrote the manuscript. H.Z., C.L.S., and C.A.M. performed *in vitro* experiments. G.F. assisted with experiments and provided critical technical input. S.N.A.H. provided experimental and intellectual input. V.A. provided intellectual input and funding support. I.L.K. conceptualized the study, designed experiments, and wrote the manuscript.

DECLARATION OF INTERESTS

The authors declare no competing interests.

Received: December 1, 2020
Revised: May 21, 2021
Accepted: July 7, 2021
Published: July 27, 2021

REFERENCES

Agard, M., Asakrah, S., and Morici, L.A. (2013). PGE(2) suppression of innate immunity during mucosal bacterial infection. Front. Cell. Infect. Microbiol. *3*, 45.

Baratelli, F., Lin, Y., Zhu, L., Yang, S.C., Heuzé-Vourc'h, N., Zeng, G., Reckamp, K., Dohadwala, M., Sharma, S., and Dubinett, S.M. (2005). Prostaglandin E2 induces FOXP3 gene expression and T regulatory cell function in human CD4+ T cells. J. Immunol. *175*, 1483–1490.

Boniface, K., Bak-Jensen, K.S., Li, Y., Blumenschein, W.M., McGeachy, M.J., McClanahan, T.K., McKenzie, B.S., Kastelein, R.A., Cua, D.J., and de Waal Malefyt, R. (2009). Prostaglandin E2 regulates Th17 cell differentiation and function through cyclic AMP and EP2/EP4 receptor signaling. J. Exp. Med. *206*, 535–548.

Brown, S.L., Riehl, T.E., Walker, M.R., Geske, M.J., Doherty, J.M., Stenson, W.F., and Stappenbeck, T.S. (2007). Myd88-dependent positioning of Ptgs2-expressing stromal cells maintains colonic epithelial proliferation during injury. J. Clin. Invest. *117*, 258–269.

Cai, Y., Shen, X., Ding, C., Qi, C., Li, K., Li, X., Jala, V.R., Zhang, H.G., Wang, T., Zheng, J., and Yan, J. (2011). Pivotal role of dermal IL-17-producing $\gamma\delta$ T cells in skin inflammation. Immunity *35*, 596–610.

Chen, Y.S., Chen, I.B., Pham, G., Shao, T.Y., Bangar, H., Way, S.S., and Haslam, D.B. (2020). IL-17-producing $\gamma\delta$ T cells protect against Clostridium difficile infection. J. Clin. Invest. *130*, 2377–2390.

Chizzolini, C., Chicheportiche, R., Alvarez, M., de Rham, C., Roux-Lombard, P., Ferrari-Lacraz, S., and Dayer, J.M. (2008). Prostaglandin E2 synergistically with interleukin-23 favors human Th17 expansion. Blood *112*, 3696–3703.

Cho, J.S., Pietras, E.M., Garcia, N.C., Ramos, R.I., Farzam, D.M., Monroe, H.R., Magorien, J.E., Blauvelt, A., Kolls, J.K., Cheung, A.L., et al. (2010). IL-17 is essential for host defense against cutaneous Staphylococcus aureus infection in mice. J. Clin. Invest. *120*, 1762–1773.

Crittenden, S., Goepp, M., Pollock, J., Robb, C.T., Smyth, D.J., Zhou, Y., Andrews, R., Tyrrell, V., Gkikas, K., Adima, A., et al. (2021). Prostaglandin E_2 promotes intestinal inflammation via inhibiting microbiota-dependent regulatory T cells. Sci. Adv. *7*, eabd7954.

Cua, D.J., and Tato, C.M. (2010). Innate IL-17-producing cells: the sentinels of the immune system. Nat. Rev. Immunol. *10*, 479–489.

Du, B., Zhu, M., Li, Y., Li, G., and Xi, X. (2020). The prostaglandin E2 increases the production of IL-17 and the expression of costimulatory molecules on $\gamma\delta$ T cells in rheumatoid arthritis. Scand. J. Immunol. *91*, e12872.

Duan, J., Chung, H., Troy, E., and Kasper, D.L. (2010). Microbial colonization drives expansion of IL-1 receptor 1-expressing and IL-17-producing gamma/delta T cells. Cell Host Microbe *7*, 140–150.

Duffin, R., O'Connor, R.A., Crittenden, S., Forster, T., Yu, C., Zheng, X., Smyth, D., Robb, C.T., Rossi, F., Skouras, C., et al. (2016). Prostaglandin E_2 constrains systemic inflammation through an innate lymphoid cell-IL-22 axis. Science *351*, 1333–1338.

Erb-Downward, J.R., and Huffnagle, G.B. (2007). Cryptococcus neoformans produces authentic prostaglandin E2 without a cyclooxygenase. Eukaryot. Cell *6*, 346–350.

Fiala, G.J., Schaffer, A.M., Merches, K., Morath, A., Swann, J., Herr, L.A., Hils, M., Esser, C., Minguet, S., and Schamel, W.W.A. (2019). Proximal *Lck* Promoter-Driven *Cre* Function Is Limited in Neonatal and Ineffective in Adult γδ T Cell Development. J. Immunol. *203*, 569–579.

Gray, E.E., Ramírez-Valle, F., Xu, Y., Wu, S., Wu, Z., Karjalainen, K.E., and Cyster, J.G. (2013). Deficiency in IL-17-committed Vγ4(+) γδ T cells in a spontaneous Sox13-mutant CD45.1(+) congenic mouse substrain provides protection from dermatitis. Nat. Immunol. *14*, 584–592.

Hellewell, P.G., Jose, P.J., and Williams, T.J. (1992). Inflammatory mechanisms in the passive cutaneous anaphylactic reaction in the rabbit: evidence that novel mediators are involved. Br. J. Pharmacol. *107*, 1163–1172.

Huang, M., Sharma, S., Mao, J.T., and Dubinett, S.M. (1996). Non-small cell lung cancer-derived soluble mediators and prostaglandin E2 enhance peripheral blood lymphocyte IL-10 transcription and protein production. J. Immunol. *157*, 5512–5520.

Jaffar, Z., Ferrini, M.E., Shaw, P.K., FitzGerald, G.A., and Roberts, K. (2011). Prostaglandin I_2promotes the development of IL-17-producing γδ T cells that associate with the epithelium during allergic lung inflammation. J. Immunol. *187*, 5380–5391.

Jain, U., Lai, C.W., Xiong, S., Goodwin, V.M., Lu, Q., Muegge, B.D., Christophi, G.P., Vandussen, K.L., Cummings, B.P., Young, E., et al. (2018). Temporal Regulation of the Bacterial Metabolite Deoxycholate during Colonic Repair Is Critical for Crypt Regeneration. Cell Host Microbe. *24*, 353–363.e5.

Jensen, K.D., Su, X., Shin, S., Li, L., Youssef, S., Yamasaki, S., Steinman, L., Saito, T., Locksley, R.M., Davis, M.M., et al. (2008). Thymic selection determines gammadelta T cell effector fate: antigen-naive cells make interleukin-17 and antigen-experienced cells make interferon gamma. Immunity *29*, 90–100.

Kalinski, P. (2012). Regulation of immune responses by prostaglandin E2. J. Immunol. *188*, 21–28.

Kashem, S.W., Riedl, M.S., Yao, C., Honda, C.N., Vulchanova, L., and Kaplan, D.H. (2015). Nociceptive Sensory Fibers Drive Interleukin-23 Production from CD301b+ Dermal Dendritic Cells and Drive Protective Cutaneous Immunity. Immunity *43*, 515–526.

Lee, J.S., Tato, C.M., Joyce-Shaikh, B., Gulen, M.F., Cayatte, C., Chen, Y., Blumenschein, W.M., Judo, M., Ayanoglu, G., McClanahan, T.K., et al. (2015). Interleukin-23-Independent IL-17 Production Regulates Intestinal Epithelial Permeability. Immunity *43*, 727–738.

Lee, J., Aoki, T., Thumkeo, D., Siriwach, R., Yao, C., and Narumiya, S. (2019). T cell-intrinsic prostaglandin E_2-EP2/EP4 signaling is critical in pathogenic T_H17 cell-driven inflammation. J. Allergy Clin. Immunol. *143*, 631–643.

Li, F., Hao, X., Chen, Y., Bai, L., Gao, X., Lian, Z., Wei, H., Sun, R., and Tian, Z. (2017). Erratum: The microbiota maintain homeostasis of liver-resident γδT-17 cells in a lipid antigen/CD1d-dependent manner. Nat. Commun. *8*, 15265.

Livak, K.J., and Schmittgen, T.D. (2001). Analysis of relative gene expression data using real-time quantitative PCR and the 2(-Delta Delta C(T)) Method. Methods *25*, 402–408.

Mabuchi, T., Singh, T.P., Takekoshi, T., Jia, G.F., Wu, X., Kao, M.C., Weiss, I., Farber, J.M., and Hwang, S.T. (2013). CCR6 is required for epidermal trafficking of γδ-T cells in an IL-23-induced model of psoriasiform dermatitis. J. Invest. Dermatol. *133*, 164–171.

Manca, C., Boubertakh, B., Leblanc, N., Deschênes, T., Lacroix, S., Martin, C., Houde, A., Veilleux, A., Flamand, N., Muccioli, G.G., et al. (2020). Germ-free mice exhibit profound gut microbiota-dependent alterations of intestinal endocannabinoidome signaling. J. Lipid Res. *61*, 70–85.

Martin, B., Hirota, K., Cua, D.J., Stockinger, B., and Veldhoen, M. (2009). Interleukin-17-producing gammadelta T cells selectively expand in response to pathogen products and environmental signals. Immunity *31*, 321–330.

McKenzie, D.R., Kara, E.E., Bastow, C.R., Tyllis, T.S., Fenix, K.A., Gregor, C.E., Wilson, J.J., Babb, R., Paton, J.C., Kallies, A., et al. (2017). IL-17-producing γδ T cells switch migratory patterns between resting and activated states. Nat. Commun. *8*, 15632.

Medeiros, A.I., Serezani, C.H., Lee, S.P., and Peters-Golden, M. (2009). Efferocytosis impairs pulmonary macrophage and lung antibacterial function via PGE2/EP2 signaling. J. Exp. Med. *206*, 61–68.

Mielke, L.A., Jones, S.A., Raverdeau, M., Higgs, R., Stefanska, A., Groom, J.R., Misiak, A., Dungan, L.S., Sutton, C.E., Streubel, G., et al. (2013). Retinoic acid expression associates with enhanced IL-22 production by γδ T cells and innate lymphoid cells and attenuation of intestinal inflammation. J. Exp. Med. *210*, 1117–1124.

Miyoshi, H., VanDussen, K.L., Malvin, N.P., Ryu, S.H., Wang, Y., Sonnek, N.M., Lai, C.Y., and Stappenbeck, T.S. (2017). Prostaglandin E2 promotes intestinal repair through an adaptive cellular response of the epithelium. EMBO *36*, 5–24.

Montrose, D.C., Nakanishi, M., Murphy, R.C., Zarini, S., McAleer, J.P., Vella, A.T., and Rosenberg, D.W. (2015). The role of PGE2 in intestinal inflammation and tumorigenesis. Prostaglandins Other Lipid Mediat. *116-117*, 26–36.

Muñoz-Ruiz, M., Ribot, J.C., Grosso, A.R., Gonçalves-Sousa, N., Pamplona, A., Pennington, D.J., Regueiro, J.R., Fernández-Malavé, E., and Silva-Santos, B. (2016). TCR signal strength controls thymic differentiation of discrete proinflammatory γδ T cell subsets. Nat. Immunol. *17*, 721–727.

Muschaweckh, A., Petermann, F., and Korn, T. (2017). IL-1β and IL-23 Promote Extrathymic Commitment of $CD27^+CD122^-$ γδ T Cells to γδT17 Cells. J. Immunol. *199*, 2668–2679.

Napolitani, G., Acosta-Rodriguez, E.V., Lanzavecchia, A., and Sallusto, F. (2009). Prostaglandin E2 enhances Th17 responses via modulation of IL-17 and IFN-gamma production by memory CD4+ T cells. Eur. J. Immunol. *39*, 1301–1312.

Papotto, P.H., Gonçalves-Sousa, N., Schmolka, N., Iseppon, A., Mensurado, S., Stockinger, B., Ribot, J.C., and Silva-Santos, B. (2017a). IL-23 drives differentiation of peripheral γδ17 T cells from adult bone marrow-derived precursors. EMBO Rep. *18*, 1957–1967.

Papotto, P.H., Ribot, J.C., and Silva-Santos, B. (2017b). $IL\text{-}17^+$ γδ T cells as kick-starters of inflammation. Nat. Immunol. *18*, 604–611.

Polese, B., Zhang, H., Thurairajah, B., and King, I.L. (2020). Innate Lymphocytes in Psoriasis. Front. Immunol. *11*, 242.

Rakoff-Nahoum, S., Paglino, J., Eslami-Varzaneh, F., Edberg, S., and Medzhitov, R. (2004). Recognition of commensal microflora by toll-like receptors is required for intestinal homeostasis. Cell *118*, 229–241.

Ribot, J.C., deBarros, A., Pang, D.J., Neves, J.F., Peperzak, V., Roberts, S.J., Girardi, M., Borst, J., Hayday, A.C., Pennington, D.J., and Silva-Santos, B. (2009). CD27 is a thymic determinant of the balance between interferon-gamma- and interleukin 17-producing gammadelta T cell subsets. Nat. Immunol. *10*, 427–436.

Ridaura, V.K., Bouladoux, N., Claesen, J., Chen, Y.E., Byrd, A.L., Constantinides, M.G., Merrill, E.D., Tamoutounour, S., Fischbach, M.A., and Belkaid, Y. (2018). Contextual control of skin immunity and inflammation by *Corynebacterium*. J. Exp. Med. *215*, 785–799.

Roulis, M., Kaklamanos, A., Schernthanner, M., Bielecki, P., Zhao, J., Kaffe, E., Frommelt, L.S., Qu, R., Knapp, M.S., Henriques, A., et al. (2020). Paracrine orchestration of intestinal tumorigenesis by a mesenchymal niche. Nature *580*, 524–529.

Sandrock, I., Reinhardt, A., Ravens, S., Binz, C., Wilharm, A., Martins, J., Oberdörfer, L., Tan, L., Lienenklaus, S., Zhang, B., et al. (2018). Genetic models reveal origin, persistence and non-redundant functions of IL-17-producing γδ T cells. J. Exp. Med. *215*, 3006–3018.

Sheibanie, A.F., Tadmori, I., Jing, H., Vassiliou, E., and Ganea, D. (2004). Prostaglandin E2 induces IL-23 production in bone marrow-derived dendritic cells. FASEB J. *18*, 1318–1320.

Sheridan, B.S., Romagnoli, P.A., Pham, Q.M., Fu, H.H., Alonzo, F., 3rd, Schubert, W.D., Freitag, N.E., and Lefrancois, L. (2013). gammadelta T cells exhibit multifunctional and protective memory in intestinal tissues. Immunity *39*, 184–195.

Shouval, D.S., Biswas, A., Goettel, J.A., McCann, K., Conaway, E., Redhu, N.S., Mascanfroni, I.D., Al Adham, Z., Lavoie, S., Ibourk, M., et al. (2014). Interleukin-10 receptor signaling in innate immune cells regulates mucosal immune tolerance and anti-inflammatory macrophage function. Immunity *40*, 706–719.

Sutton, C.E., Lalor, S.J., Sweeney, C.M., Brereton, C.F., Lavelle, E.C., and Mills, K.H. (2009). Interleukin-1 and IL-23 induce innate IL-17 production from gammadelta T cells, amplifying Th17 responses and autoimmunity. Immunity *31*, 331–341.

Valdez, P.A., Vithayathil, P.J., Janelsins, B.M., Shaffer, A.L., Williamson, P.R., and Datta, S.K. (2012). Prostaglandin E2 suppresses antifungal immunity by inhibiting interferon regulatory factor 4 function and interleukin-17 expression in T cells. Immunity *36*, 668–679.

van der Fits, L., Mourits, S., Voerman, J.S., Kant, M., Boon, L., Laman, J.D., Cornelissen, F., Mus, A.M., Florencia, E., Prens, E.P., and Lubberts, E. (2009). Imiquimod-induced psoriasis-like skin inflammation in mice is mediated via the IL-23/IL-17 axis. J. Immunol. *182*, 5836–5845.

Viennois, E., Chen, F., Laroui, H., Baker, M.T., and Merlin, D. (2013). Dextran sodium sulfate inhibits the activities of both polymerase and reverse transcriptase: lithium chloride purification, a rapid and efficient technique to purify RNA. BMC Res. Notes *6*, 360.

Wedmore, C.V., and Williams, T.J. (1981). Control of vascular permeability by polymorphonuclear leukocytes in inflammation. Nature *289*, 646–650.

Yao, C., Sakata, D., Esaki, Y., Li, Y., Matsuoka, T., Kuroiwa, K., Sugimoto, Y., and Narumiya, S. (2009). Prostaglandin E2-EP4 signaling promotes immune inflammation through Th1 cell differentiation and Th17 cell expansion. Nat. Med. *15*, 633–640.

Zhang, H., Carnevale, G., Polese, B., Simard, M., Thurairajah, B., Khan, N., Gentile, M.E., Fontes, G., Vinh, D.C., Pouliot, R., and King, I.L. (2019). CD109 Restrains Activation of Cutaneous IL-17-Producing γδ T Cells by Commensal Microbiota. Cell Rep. *29*, 391–405.e5.

Zuberbuehler, M.K., Parker, M.E., Wheaton, J.D., Espinosa, J.R., Salzler, H.R., Park, E., and Ciofani, M. (2019). The transcription factor c-Maf is essential for the commitment of IL-17-producing γδ T cells. Nat. Immunol. *20*, 73–85.

STAR★METHODS

KEY RESOURCES TABLE

REAGENT or RESOURCE	SOURCE	IDENTIFIER
Antibodies		
Mouse monoclonal anti-mouse CD45.2-PE-eFluor 610 (104)	Thermofisher	Cat# 61-0454-82; RRID: AB_2574562
Hamster monoclonal anti-Mouse CD3e-BV650 (145-2C11)	BD	Cat# 564378; RRID: AB_2738779
Hamster monoclonal anti-Mouse TCRβ-APC-eFluor 780 (H57-597)	Thermofisher	Cat# 47-5961-8; RRID: AB_1272173
Hamster monoclonal anti-Mouse TCRδ-FITC (GL3)	Biolegend	Cat# 118106; RRID: AB_313830
Hamster monoclonal anti-Mouse TCRδ-PE (GL3)	Biolegend	Cat# 118108; RRID: AB_313832
Hamster monoclonal anti-Mouse TCRδ-PerCP/Cy5.5 (GL3)	Biolegend	Cat# 118118; RRID: AB_10612756
Hamster monoclonal anti-Mouse TCR Vγ2(4)-PE-Cyanine7 (UC3-10A6)	Thermofisher	Cat# 25-5828-82; RRID: AB_2573474
Hamster monoclonal anti-Mouse TCR Vγ2(4)-PE (UC3-10A6)	Biolegend	Cat# 137706; RRID: AB_10643577
Rat monoclonal anti-mouse IL-17a-PE (eBio17B7)	Thermofisher	Cat# 12-7177-81; RRID: AB_763582
Rat monoclonal anti-mouse IFN-γ-Alexa Fluor 488 (XMG1.2)	Thermofisher	Cat# 53-7311-82; RRID: AB_469932
Rat monoclonal anti-mouse IL-22-PE (1H8PWSR)	Thermofisher	Cat# 12-7221-82; RRID:AB_10597428
Rat monoclonal anti-mouse IL-17F-AF488 (18F10)	Thermofisher	Cat# 53-7471-82; RRID:AB_1210529
Rat monoclonal anti-mouse IL-10-BV421 (JES5-16E3)	BD	Cat# 563276; RRID:AB_2738111
Rat monoclonal anti-mouse c-Maf-eFluor660 (sym0F1)	Thermofisher	Cat# 50-9855-82; RRID:AB_2574388
Rat monoclonal anti-mouse IRF4-PE-Cy7 (3E4)	Thermofisher	Cat# 25-9858-82; RRID:AB_2573558
Rat monoclonal anti-mouse Rorγt-APC (B2D)	Thermofisher	Cat# 17-6981-82; RRID:AB_2573254
Rat monoclonal anti-mouse IL-1R-APC (JAMA-147)	Biolegend	Cat# 113509; RRID:AB_2264757
Rat monoclonal anti-mouse IL-23R-PE (12B2B64)	Biolegend	Cat# 150904; RRID:AB_2572189
Rat monoclonal anti-mouse CD127-PE (A7R34)	Thermofisher	Cat# 12-1271-82; RRID:AB_465844
Rabbit polyclonal anti-mouse EP2-Fitc	Alomone	Cat# APR-064-F; RRID:AB_2827348
Rat monoclonal anti-mouse CD11b-APC (M1/70)	Thermofisher	Cat# 17-0112-82; RRID: AB_469343
Rat monoclonal anti-mouse MHCII-Fitc (M5/114.15.2)	Thermofisher	Cat# 11-5321-85; RRID:AB_465233
Rat monoclonal anti-mouse Foxp3-AF700 (FJK-16 s)	Thermofisher	Cat# 56-5773-82; RRID:AB_1210557
Rat monoclonal anti-mouse Ly6G-Alexa Fluor 488 (1A8-Ly6g)	Thermofisher	Cat # 11-9668-82; RRID:AB_2572532

(*Continued on next page*)

Continued

REAGENT or RESOURCE	SOURCE	IDENTIFIER
Rat monoclonal anti-mouse CD3 (145-2C11)	Thermofisher	Cat# 16-0031-85; RRID:AB_468848
Rat monoclonal anti-mouse CD28 (37.51)	Thermofisher	Cat# 16-0281-85; RRID:AB_468922
Bacterial and virus strains		
Corynebacterium accolens	ATCC	Cat# 49725
Chemicals, peptides and recombinant peptides		
Recombinant mouse IL-23	Biolegend	Cat# 589004
Recombinant mouse IL-1β	Biolegend	Cat# 575102
Prostaglandin E_2	Cayman Chemical	Cat#14010
16-16-dimethyl Prostaglandin E_2	Cayman Chemical	Cat#14750
Fixable Viability Dye-eFluor 506	eBioscience	Cat# 65-0866-18
Fixable Viability Dye-eFluor 780	eBioscience	Cat# 65-0865-18
Fixation/Permeabilization Concentrate	eBioscience	Cat# 00-5123-43
Fixation/Permeabilization Diluent	eBioscience	Cat# 00-5223-56
Permeabilization Buffer (10X)	eBioscience	Cat# 00-8333-56
Collagenase from *Clostridium histolyticum* (Collagenase, Type IV)	Sigma-Aldrich	Cat# C5138
DNase I	Roche	Cat# 11284932001
Collagenase/Dispase	Sigma-Aldrich	Cat# 11097113001
PMA	Sigma-Aldrich	Cat# P1585
Ionomycin calcium salt from *Streptomyces conglobatus*	Sigma-Aldrich	Cat# I0634
EDTA (Ethylene diamine tetra acetic acid) disodium salt	BDH	Cat# ACS 345
RPMI 1640 Medium	GIBCO	Cat# 11875119
HBSS, calcium, magnesium	GIBCO	Cat# 24020117
DPBS, no calcium, no magnesium	GIBCO	Cat# 14190144
FBS (fetal bovine serum)	Wisent	Cat# 081-105
EvaGreen 2X qPCR mastermix without ROX	ABM	Cat# ABMMmix-S-XL
DNase/RNase-Free Distilled Water	Invitrogen	Cat# 10977015
3.75% Imiquimod (Zyclara) cream	Valeant	DIN 02340445
3% Dextran Sodium Sulfate	MP Biomedicals	Cat# 9011-18-1
Corynebacterium accolens	ATCC	Cat# 49725
BHI broth	Millipore	Cat# **53286**
Butaprost	Cayman Chemical	Cat# 13740
Sulprostone	Cayman Chemical	Cat# 14765
AH23848	Cayman Chemical	Cat# 19023
Misoprostol	Cayman Chemical	Cat# 13820
Critical commercial assays		
IL-17A Mouse Uncoated ELISA Kit	Invitrogen	Cat# 88-7371-88
DNeasy Blood & Tissue Kit	QIAGEN	Cat# 69506
RNeasy Mini Kit	QIAGEN	Cat# 74104
Prostaglandin E_2 ELISA	Cayman Chemical	Cat# 500141
Hemoccult	Beckman Coulter	Cat# 64151
Experimental models: Organisms/strains		
Mouse: C57BL/6 (B6)	Jackson Lab	Stock No: 000664 | Black 6
Mouse: *Pgtes*−/−	Maziar Divangahi	PMC4385488
Mouse: B6.129P2(Cg)-Rorc^{tm2Litt}/J	Jackson lab	Stock No: 007572 | Rorc(γt)-EGFP

(*Continued on next page*)

Continued

REAGENT or RESOURCE	SOURCE	IDENTIFIER
Software and algorithms		
GraphPad Prism 7	GraphPad Software	https://www.graphpad.com
FlowJo	BD	https://www.flowjo.com
Other		
Pulse oximeter	Kent Scientific	Cat# MSTAT-Jr

RESOURCE AVAILABILITY

Lead contact

Further information and requests for resources and reagents should be directed to and will be fulfilled by the lead contact, Irah L. King (irah.king@mcgill.ca).

Materials availability

This study did not generate new unique reagents.

Data and code availability

This study did not generate particular type of datasets/code.

EXPERIMENTAL MODEL AND SUBJECT DETAILS

Animals

C57BL/6 and *Ptges*−/− male and female mice (8-12 weeks old) on a C57BL/6 background were bred and used under specific pathogen-free conditions at the Animal Resource Division at the McGill University Health Centre – Research Institute. In all studies involving *Ptges*−/− and *Ptges*+/+ mice, littermates were used as controls. RORγt-GFP/+ used contain one wild-type RORγt allele and express GFP in all RORγt expressing cells. All animal studies were approved by the McGill University Health Centre – Research Institute Animal Resources Division (protocol 7977).

Bacteria

Corynebacterium accolens strain 49725 (ATCC) was cultured for in BHI broth (BD) supplemented with 1% Tween 80 at 37°C.

METHOD DETAILS

Cell stimulation and culture

To prepare single cell suspensions from peripheral lymph nodes, tissues were crushed through a 70 μm cell strainer using a syringe plunger and rinsed with RPMI 1640 media containing R10 media (RPMI 1640 supplemented with 10% FBS, 15mM HEPES, 1% L-glutamine and 1% Penicillin/Streptomycin). For purified T cell cultures, total CD3+ T cells were isolated from skin-draining lymph nodes using the EasySep Mouse T cell isolation kit (STEMCELL Technologies). For pure γδ T cell cultures, γδ T cells were isolated from skin-draining lymph nodes using the PE EasySep Mouse PE Positive Selection Kit II (STEMCELL Technologies) with an anti-TCRδ-PE antibody (Biolegend). Cells were cultured for 4, 8 or 18 hours under various conditions with R10 media; IL-1β (Biolegend) and IL-23 (Biolegend) were both used at 10ng/ml. PGE_2 (Cayman) was used at 1 μM except for dose-response experiments as indicated. EP agonists ((Butaprost as EP2 agonist, Sulprostone as an EP1 and EP3 agonist, EP4 agonist (AH 23848) and Misoprostol (PGE_2 analog stimulating all EP receptors)) were used at 10 μM (Cayman Chemicals). For CD3/CD28 stimulation, 24-well plates were coated overnight at 4°C with PBS containing 1ug/ml anti-mouse CD3e (eBioscience) and 1ug/ml anti-mouse CD28. Before plating, wells were rinsed with PBS. For skin cell and colon cell culture, 1×10^6 cells/well were cultured in 24 well plates containing R10 media for 18 hours with 10ng/ml IL-1β and IL-23 and 1 μM PGE_2. Golgi stop (0.67ul/ml) was added during the last 4 hours in order to study cytokine production. At the end of the culture, supernatants were collected and processed for cytokine detection by ELISA. Cells were washed twice with PBS before processing for RNA extraction or FACS analysis.

Skin cell isolation

To prepare single cell suspensions from skin tissue, ears were cut across the hairline and manually separated into rostral and caudal sides using tweezers. To separate the epidermis from the dermis, each side was incubated dermal side down in separation buffer (RPMI 1640 containing 1mg/ml Collagenase/Dispase) for 1.5 hours at 37°C. The epidermis and dermis were then rinsed in cold PBS, cut into small pieces and incubated with digestion buffer (RPMI 1640 containing 150 U/ml Collagenase IV, 200 U/ml DNase I and 2% FBS) for 2 hours at 37°C. For spontaneous cytokine detection by flow cytometry, the protein transport inhibitor Golgi

stop (BD bioscience) was added into the digestion buffer (0.67 μL Golgi stop/ml of buffer). Following incubation, the tissue was pipetted up and down in the digestion buffer to generate a single cell suspension, then passed through a 100 μm cell strainer. Cells were washed and resuspended in R10 buffer prior to culture or flow cytometry analysis.

C. accolens culture and administration

Corynebacterium accolens strain 49725 (ATCC) was plated from a frozen stock onto a brain–heart infusion (BHI) agar (BD) plate supplemented with 1% Tween (Sigma-Aldrich) overnight at 37°C. In the morning, one colony was cultured for ~5 hours in BHI broth (BD) supplemented with 1% Tween 80 at 37°C. Bacteria were enumerated before topical application by measuring OD at 600 nm with the use of a spectrophotometer and by assessing CFUs by plating serial dilutions. A concentration of $\sim 10^8$ CFU/ml was used for topical application. Five ml of *C. Accolens* broth suspension or vehicle control (broth alone) was applied on the whole skin and ears of mice every other day for eight days under anesthesia using a sterile cotton swab. Control mice were left untreated. Ears and skin draining lymph nodes were harvested on the ninth day. After isolation, cells were stimulated with PMA (50ng/ml) and Ionomycin (1 μg/ml) in R10 media and Golgi stop for 3 hours before intracellular staining and FACS analysis.

Bone marrow-derived macrophage cultures

Femurs from C57BL/6 mice were dissected and cleared of surrounding muscle in cold PBS. Bone marrow cells were flushed in non-differentiating media (RPMI 1640 containing 10%FBS and 1% Pencilli/Streptomycin), and centrifuged at 1800rpm for 5 minutes at 4°C. Red blood cells were lysed with 1X Red Blood Cell Lysis Buffer for 2-3 minutes, cells were washed, and resuspended. 5-10x10^6 bone marrow cells were seeded in a 10cm Petri Dish containing 15mL of differentiating media (RPMI 1640 containing 10%FBS, 1% Penicillin/Streptomycin, and 20% L929 Cell Conditioned Medium). Three days later, dishes were supplemented with 10mL of differentiating media. On day 6 of culture, differentiated BMDMs were washed with PBS several times, detached using Cell Stripper, and plated in the desired format for stimulation in non-differentiating media. Cells were allowed to adhere overnight prior to stimulation with heat-killed *E. coli*.

Colon cell isolation

To prepare single cell suspensions from colon tissue, mesenteric fat was removed, the tissue was cut longitudinally and washed in cold PBS. The tissue was cut in 1 cm pieces, placed in 15mL of pre-warmed HBSS+EDTA buffer (Hank's Balanced Salt Solution [HBSS] supplemented with 5mM EDTA, 10% Fetal Bovine Serum [FBS] and 15mM HEPES) and incubated at 37°C, shaking at 250 rpm for 20 minutes. The tissue was filtered through a 100 μm filter in order to remove the intraepithelial lymphocytes and epithelial cells, and this process was repeated a second time. The tissue was then washed twice with 15mL of cold HBSS buffer (HBSS supplemented with 2% FBS and 15mM HEPES). Following the second wash, buffer was decanted, and excess liquid was removed with absorbent wipes. The tissue was digested in 5mL of digestion buffer (RPMI 1640 supplemented with 10% FBS, 15 mM HEPES, 100U/mL of DNase and 400U/mL of Collagenase VIII) for 35 minutes at 37°C, with shaking at 250 rpm. The digestion was stopped by adding 35 mL of cold R10 buffer. The tissue was passed through a 100 μm filter and centrifuged at 2500 rpm for 10 minutes at 4°C. The cells were then re-suspended in R10 buffer and counted.

Imiquimod-induced skin inflammation

The back skin of 8-12 week old mice was shaved and topically treated with 50mg of 3.75% Imiquimod cream or Zyclara (Valeant) for 5 consecutive days. Control mice were left untreated. To quantitatively assess skin thickening, ears were treated with 6-8mg of Zyclara for 5 consecutive days and thickness was measured daily by a digital Vernier caliper (accuracy: 0.01mm, Proster). Researchers were aware of group allocation. Mice were sacrificed on the sixth day for tissue processing. In some experiments, mice were daily injected intraperitoneally with 200ul of stable PGE2 (16,16-dimethyl PGE2, 50 μg/ml; Cayman chemicals) or vehicle (ethanol) solution beginning at day 0 of IMQ application. Pictures to check vascularization were taken at the indicated time point while mice were anesthetized following PGE_2 injection. Oxygen saturation of the hind paw was measured using a PhysioSuite monitor with mouse paw pulse oximeter sensor attachment (Kent Scientific).

PGE_2 quantification

Back skin and colon (2cm) were harvested and flash frozen in liquid nitrogen. Samples were stored at −80°C until extraction. Tissue was weighed and placed in buffer (0.1M sodium phosphate with 1mM EDTA and 10 μM indomethacin). Tissue was homogenized on ice. Lysates were centrifuged at 10,000 rpm for 10 minutes and supernatants were collected and stored at −20°C. Ethanol precipitation was performed on samples by adding 100 μL of sample to 400 μL of ethanol. Samples were centrifuged at 10,000 rpm for 5 minutes, supernatant was collected and placed in a CentriVap vacuum concentrator (Labconco) until ethanol completely evaporated. Samples were then resuspended in 100 μL of sodium phosphate buffer and PGE_2 was detected using a monoclonal antibody ELISA kit (Cayman).

Dextran sodium sulfate treatment

Mice were given 3% DSS in drinking water (or water only for controls) for indicated time before sacrifice. Mice were monitored daily for weight loss and blood in the feces. Researchers were aware of group allocation. Hemoccult colorimetric SENSA kit

(Beckman Coulter) was used to assess rectal bleeding by treating fecal smears with H_2O_2/Ethanol treatment and observing activation of a blue compound. The following method to score the severity of intestinal bleeding: 0, no detection blue dye; 1, detection of faint blue color within ten seconds; 2, detection of pale blue color within five seconds; 3, detection of dark blue color within ten seconds; 4, detection of dark blue color within five seconds; 5, visibly red stool. On the day of sacrifice, colons were harvested and the last cm was fixed in 10% formalin for histological analyses. Remaining colonic tissue was used for cell isolation and FACS analysis. In some experiments, mice were daily injected intraperitoneally with 200ul of stable PGE_2 (16,16-dimethyl PGE_2, 1 μg/ml; Cayman chemicals) or vehicle (ethanol) solution beginning 1 day prior to start of DSS treatment.

Antibiotic treatment

Mice were given a solution of 1mg/ml of neomycin, 1mg/ml ampicillin, 1mg/ml gentamycin, 1mg/ml metronadizole, 0.5mg/ml vancomycin in the drinking water for four weeks (changed every 4 days). 16S depletion was confirmed using DNA extraction and qPCR on stool samples prior to DSS treatment.

Flow cytometry

After *ex vivo* isolation or culture, cells were washed in PBS prior to staining. For extracellular staining, single cell suspensions were incubated with fixable viability dye in 100 μL PBS (eBioscience), washed and incubated with anti-Fc receptor (clone 2.4G2, BD biosciences) for 10 minutes before adding fluorochrome-labeled antibodies at pre-determined concentrations in 100 μL FACs buffer (PBS containing 2% FBS and 10mM HEPES) for 30 minutes on ice. For intracellular staining, cells were fixed after extracellular staining with the Intracellular fixation/permeabilization buffer (eBioscience) according to the manufacturer's instructions followed by antibody labeling in 100 μL permeabilization buffer. After intracellular labeling, cells were washed and resuspended in 300 μL FACS buffer. Data were acquired on an LSR Fortessa (BD Biosciences) and analyzed with FlowJo software.

Quantitative RT-PCR and ELISA

All samples were processed for RNA extraction using QIAGEN RNeasy Mini Kit as per the manufacturer's instructions. For studies involving purified γδ T cells, the RNeasy Micro Kit was used. Equal amounts of RNA from each sample were processed into cDNA using the QuantiTect Reverse Transcription Kit (Thermofisher). Primers for *Hprt,* Fwd: AGGACCTCTCGAAGTGTTGG, Rev: AACTTGCGCTCATCTTAGGC; *Il17a,* Fwd: ACTCTCCACCGCAATGAAGA, Rev: CTCTCAGGCTCCCTCTTCAG and *Il1b*, Fwd: GGGCCTCAAAGGAAAGAATC, Rev: TACCAGTTGGGGAACTCTGC were specifically designed for the target genes. Relative expression of genes of interest was measured by real-time quantitative PCR with Brightgreen 2X qPCR master mix (ABM). Target gene expression was normalized to *Hprt* and expressed as fold change using the ΔΔCt formula (Livak and Schmittgen, 2001). Cell supernatants were collected and tested for mouse IL-17A using ELISA kits (Invitrogen) accordingly to manufacturer's instructions.

Histology

Skin and colon tissue were fixed in 10% formalin, paraffin embedded, sectioned and stained with hematoxylin and eosin by the MUHC-RI Histology Core. Images were taken with a BX50 Bright Field microscope (Olympus) at 10 or 20X magnification.

QUANTIFICATION AND STATISTICAL ANALYSIS

All experiments were replicated. There was no exclusion of animals or data points in this study. Animals were randomly allocated to control or treatment groups. Researchers were aware of group allocation during the experiments and the analyses. Data were analyzed with Graphpad Prism 7. Wilcoxon non-parametric paired t test, Mann-Whitney non-parametric unpaired t test or two-way ANOVA followed by Sidak's multiple comparisons test were used to determine statistical significance when appropriate. Mean or Mean with SD are shown in the graphs. Statistical test used and what n represents are indicated in the figure legends. *$p < 0.05$, **$p < 0.01$ and ***$p < 0.001$.